Democratic Republic of Algeria
Ministry of
Higher Education and
Scientific Research

Amar Telidji- Laghouat
University

FACULTY of TECHNOLOGY
MECHANICAL ENGINEERING DEPARTMENT

A dissertation submitted in partial fulfillment for the requirements of the degree of master in mechanical engineering

Presented By:
DJERIBIA Nour Elhouda
SAHARA Ali

DOMAIN: SCIENCES and TECHNOLOGIES

OPTION: ENERGETIC

Theme:

Study on Three-Dimensional Numerical Simulation of Cross-Flow Heat Exchanger: Parametric Study

Defense jury:

Member	**Quality**
Mr. BENSAYAH Khaled	**President**
Mr. BELAHCEN Lahcene	**Examiner**
Mr. HACHANI Lakhdar	**Supervisor**

College Year: 2023/2024

Dedication

Alhamdulillah

I dedicated this work to
the dearest people in my life: To the two candles
who enlightened me in my life: ***my mother*** *and* ***my father****, who*
gave me always surrounded and motivated to constantly
become better.
To ***my brothers*** *who have always been by my side and with*
whom I have shared the best moments of my life
To ***my friends*** *who accompanied me throughout my academic*
journey

To all professors of mechanical engineering department
and especially
my Supervisor Pr: ***Hachani Lakhdar****.*
To him who was with me by his encouragement
and helped me to the completion of this work.

Ali Sahara.

Dedication

I dedicated this work
To my dear parents no tribute could live up
to the love they don't stop filling me with the happiness
may God give them good health and long life.
To my dear sisters and to Hanane for their tenderness,
complicity and their encouragement.
To all my family and all my friends.

Djeribia Nour Elhouda

Abstract:

This work primarily uses Ansys/Fluent CFD software to do a thorough 3D predictive numerical simulation in a stationary regime in order to study the heat transfer capabilities of a cross-flow heat exchanger. The main objective was to conduct a comparative analysis of four different cases by varying the fluid entry velocity (oil and water) and the set pipe layout of the heat exchanger, specifically focusing on in-line and staggered configurations. In order to do this, we looked at the heat exchanger's temperature distribution and fluid flow patterns. We also estimated the energy consumption and heat transfer rate to determine the heat exchanger's efficiency. We were able to cover the optimal design for thermal efficiency.

keywords: heat exchanger – Tube Banks – CFD software (ANSYS)- Numerical simulation

Résumé :

Ce travail utilise principalement le logiciel Ansys/Fluent CFD pour effectuer une simulation numerique predictive 3D approfondie en regime stationnaire afin d'etudier les capacites de transfert de chaleur d'un **e**changeur de chaleur a flux croise**s**. L'objectif principal **t**ait de mener une analyse comparative de quatre cas differents en faisant varier la vitesse d'entre**e** du fluide (huile et eau) et la disposition des tuyaux de l'e changeur de chaleur, en se concentrant specifiquement sur les configurations en ligne et de calees. Pour ce faire, nous avons examine la re partition de la tempe rature et les sche mas d'e coulement des fluides de l 'échangeur de chaleur. Nous avons e galement estime la consommation d'e nergie et le taux de transfert de chaleur pour determiner l'efficacite de l'echangeur de chaleur. Nous avons pu couvrir la conception optimale pour l'efficacite thermique.

Mots-clés : echangeur de chaleur - Banques de tubes - Ansys/Fluent - Simulation numérique

ملخص:

يستخدم هذا العمل في المقام الأول برنامج Ansys/Fluent CFD لإجراء محاكاة عددية تنبؤية ثلاثية الأبعاد شاملة في نظام ثابت من أجل دراسة قدرات نقل الحرارة لمبادل حراري ذو تدفق متقاطع. كان الهدف الرئيسي هو إجراء تحليل مقارن لأربع حالات مختلفة عن طريق تغيير سرعة دخول السائل (الزيت والماء) وتصميم الأنابيب المحدد للمبادل الحراري، مع التركيز بشكل خاص على التكوينات الخطية والمتداخلة. القيام بذلك، نظرنا إلى توزيع درجة حرارة المبادل الحراري وأنماط تدفق السوائل. قمنا أيضًا بتقدير استهلاك الطاقة ومعدل انتقال الحرارة لتحديد كفاءة المبادل الحراري. تمكنا من تغطية التصميم الأمثل للكفاءة الحرارية.

الكلمات المفتاحية:مبادل حراري - البنوك من الأنابيب -محاكاة عددية

SUMMARY

LIST OF FIGURES

List of tables:

NOMENCLATURE

SYMBOLES	PARAMETER	UNITE
T	Temperature	°C, °K
$T_{h,in}$	Temperature of hot fluid in the inlet	°C, °K
$T_{h,out}$	Temperature of hot fluid in the outlet	°C, °K
$T_{c,out}$	Temperature of cold fluid in the outlet	°C, °K
$T_{c,in}$	Temperature of cold fluid in the inlet	°C, °K
ΔT_{LM}	Log mean deference temperature	°C, °K
ΔT_{max}	Maximum deference of temperature	°C, °K
Q	Amount of heat	W
mi_h	Mass flow rate for the hot fluid	kg/s
mi_c	Mass flow rate for the cold fluid	kg/s
mi	Mass flow rate	kg/s
m	Mass	kg
cp_h	Specific heat for the hot *fluid*	J/Kg. °C
cp_c	Specific heat for the cold fluid	J/Kg. °C
U	Overall heat transfer coefficient	$W/m^2.K$
h	Heat transfer coefficient	$W/m^2.K$
A	Heat transfer surface area	m^2
A_w	Heat transfer area of the wall	m^2

R_w	Wall thermal resistance	m^2K/W
$Qmax$	Maximum possible heat transfer rate	W
d_i and d_o	Inner and outer diameters of the circular	m
L	Tube length	m
P	perimeter	m
δ_w	Thickness of the wall	m
ρ	Density of the fluid	Kg/m^3
u_m, v	Velocity	m/s
μ	Absolute viscosity	Pa. s
K_w	Thermal conductivity of the wall	W/m. K
λ	Thermal conductivity	W/m. K
C_{min}	Minimum value of the thermal capacity rate	W/°C
C_{max}	Maxim value of the thermal capacity rate	W/°C
P_k	Turbulence production term	W/m3
ϵ	Dissipation rate of turbulent kinetic energy	W/kg
μ_t	Turbulent viscosity	Pa. s
ST	Transvers pitch	m
SL	Longitudinal pitch	m
Re	Reynolds number	
Nu	Nusselt number	
pr	Prandtl number	
ε	The heat exchanger effectiveness	
Cr	The heat capacity ratio	

General Introduction

General Introduction

Heat exchangers are important components in industrial processes as they facilitate the transfer of thermal energy between fluids. They come in different types, sizes, and shapes and are categorized based on factors like their design, operating principles, and types of heat transfer mechanisms involved.

The purpose of this numerical investigation is to use Computational Fluid Dynamics (CFD) software (ANSYS/Fluent), to numerically analyze the thermal and efficiency of crossflow heat exchanger in a stationary regime, and to identify the dominant factors influencing heat transfer within the system. Moreover, this study includes a comparison between two configurations of tubes arrangement, i.e. In-Line and staggered with different fluids (oil and water).

This dissertation is composed of three chapters. The first chapter provides a comprehensive classification overview of heat exchangers, including direct and indirect transfer types, different configuration of crossflow heat exchangers and also shell-tube exchangers, plate exchangers, and more. This chapter also introduces the LMTD method, which calculates the log mean temperature difference between hot and cold fluids within a heat exchanger, and discusses the assumptions, limitations, and procedures for its implementation. Additionally, the chapter covers factors affecting the LMTD and offers guidelines for selecting appropriate values for correction factors used in the LMTD method. Furthermore, the overall heat transfer coefficient and its conjunction with the LMTD method in computing the heat transfer rate are discussed. The ε-NTU method and its practical application in designing and analyzing heat exchangers are also presented.

The second chapter will be focused on the most important steps in terms of geometry construction, the different functions used for mesh adaptation, and the setup stage of the calculation, as well as the necessary equations used in modeling the phenomena, are also discussed in detail in this chapter.

The third chapter focuses on the discussion and comparative analysis of numerical results obtained from four different cases of crossflow heat exchangers. These cases involve water and oil as a heat transfer fluid and two distinguished arrangements of bundle of tubes (In-Line and staggered). The effect of flow regime on the heat transfer performances within the heat exchanger are also examined in terms of increasing the velocity in the shell side twenty times. The objective of this analysis is to evaluate the overall heat transfer characteristics of each type of tube arrangement in terms of temperature field, dynamic field, and thermal efficiency. The analysis considers various performance metrics, such as the heat transfer coefficient and overall heat transfer rate, and the results are presented and compared through visualizations, including contours, charts, and streamlines.

Chapter 01

Generality on heat exchangers

I.1.INTRODUCTION

An apparatus that permits heat to move from a source to a heat sink is called a heat exchanger. Without fluid mixing, this exchange can take place through a solid wall. This approach is typically used to heat or cool a liquid or gas that would be difficult or impossible to chill directly. Numerous industrial applications heavily rely on the heat exchange approach that uses heat exchangers as equipment. The physical phenomena that heat exchangers facilitate is still not entirely understood, despite the fact that the calculation, sizing, and optimization of heat exchangers remain active study areas due to their straightforward and well-known operating principle.

Therefore, we will highlight classifications of heat exchangers, and techniques for analyzing and Calculating heat exchangers. This will be the objective of the present chapter.

I.2. CLASSIFICATION OF HEAT EXCHANGERS

I.2.1. Classification according to transfer processes :

Heat exchangers are classified according to transfer processes into indirect and direct contact types.

I.2.1.1 Indirect-contact heat exchangers

In an indirect-contact heat exchanger, the fluid streams remain separate and the heat transfers continuously through an impervious dividing wall or into and out of a wall in a transient manner. Thus, ideally, there is no direct contact between thermally interacting fluids. This type of heat exchanger also referred to as a surface heat exchanger, [1].

I.2.1.2 Direct-contact heat exchangers

In a direct-contact exchanger, two fluid streams come into direct contact, exchange heat and are then separated. Common applications of a direct-contact exchanger involve mass transfer in addition to heat transfer, such as in evaporative cooling and rectification applications involving only sensible heat transfer are rare the enthalpy of phase change in such an exchanger generally represents a significant portion of the total energy transfer the phase change generally enhances the heat transfer rate. Compared to indirect contact recuperators and regenerators, in direct-contact heat exchangers (1) Very high heat transfer rates are achievable, (2) the exchanger construction is relatively in expensive and (3) the fouling problem is generally nonexistent, due to the absence of a heat transfer surface (wall)between the two fluids, [1].

I.2.1.2.1. Immiscible fluid exchangers

In this type, two immiscible fluid streams are brought into direct contact. These fluids may

Be single-phase fluids or they may involve condensation or vaporization. condensation of organic vapors and oil vapors with water or air are typical examples, [1].

I.2.1.2.2. Gas-liquid Exchangers

In this type, one fluid is a gas (more commonly, air) and the other a low-pressure liquid (more commonly, water) and are readily separable after the energy exchange, In either cooling of liquid(water) or humidification of gas (air) applications, liquid partially evaporates and the vapor is carried away with the gas in these exchangers, more than 90% of the energy transfer is by virtue of mass transfer (due to the evaporation of the liquid), and convective heat transfer is a minor mechanism A" wet" (water) cooling tower with forced- or natural-draft airflow is the most common application. Other application is the air-conditioning spray chamber, [1].

I.2.1.2.3 Liquid- Vapor Exchangers

In this type, typically steam is partially or fully condensed using cooling water, or water is heated with waste steam through direct contact n the exchanger. Non condensable and residual steam and hot water are the outlet steams. Common examples are desuperheaters and open feed water heaters (also known as deaerators) in power plants, [1].

I.2.2. Classification according to type of exchange

heat exchangers are distinguished based on the number of phases of the fluids involved:

I.2.2.1. Single-phase heat exchangers

These heat exchangers deal with fluids that remain in a single phase throughout the heat exchange process. For example, in a heat exchanger used for cooling water in an air conditioning system, the water remains in the liquid state throughout the process. Similarly, in a heat exchanger where hot air is used to heat ambient air, both air streams remain in the gaseous state.

I.2.2.2. Two-phase heat exchangers

These heat exchangers involve fluids that transition from one state to another during the heat exchange process. For example, in a water vapor condenser, water vapor condenses into liquid while releasing heat to another fluid, often water or air. Similarly, in an evaporator, a liquid may evaporate to become vapor while absorbing heat from another fluid.

These two types of heat exchangers have specific applications based on heat transfer needs and the properties of the fluids involved. Two-phase heat exchangers are often used in processes involving phase changes, such as condensation, vaporization, or sublimation, while single-phase heat exchangers are commonly used in applications where fluids remain in a single phase.

I.2.3. Classification according to flow arrangement

Based on the heat exchanger's shape and the relative directions in which the two fluids (cold and hot) flow, this categorization has been made. We simply depict the fluid flow patterns that are most frequently found in the following.

I.2.3.1 Same direction "co-current flow"

In a co-current flow heat exchanger, both the hot and cold fluids flow in the same direction, parallel to each other where the temperature of the cold fluid cannot be higher than the outlet temperature of the hot fluid sees figure (I.1). This arrangement results in a simple and compact design. However, the temperature difference between the two fluids decreases along the length of the heat exchanger, leading to lower heat transfer rates compared to other arrangements, [2].

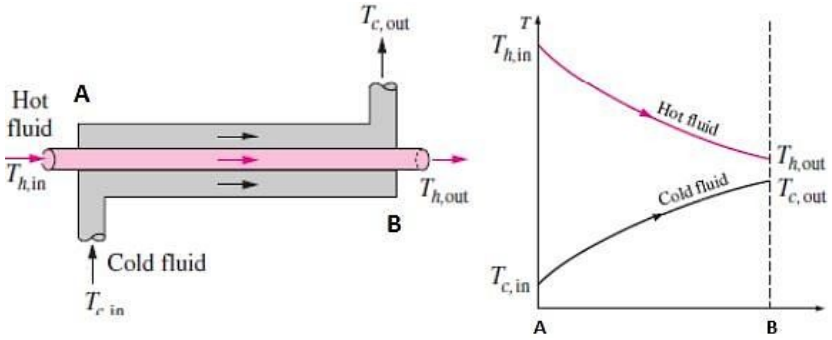

(a) (b)

Figure I.1: *Flow direction in a co-current heat exchanger(a) and temperature profile in a co-current heat exchanger (b).*

I.2.3.2 Opposite direction "counter-current flow"

In a counter-current flow heat exchanger as illustrated in figure (I.2), the hot and cold fluids flow in opposite directions, counter to each other where the temperature of the cold fluid can exceed the outlet temperature of the hot fluid.

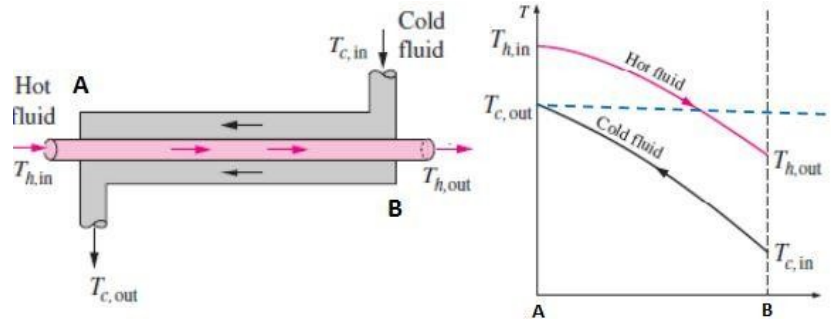

(a) (b)

Figure I.2: *Flow direction in a counter-current heat exchanger (a) and temperature profile in a counter-current heat exchanger*

This arrangement maximizes the temperature difference between the two fluids, resulting in higher heat transfer rates and efficiency compared to parallel flow. Counterflow heat exchangers are commonly used when maximum heat transfer is desired, [2].

I.2.3.3 Crossflow

In a crossflow heat exchanger, one fluid flows perpendicular to the other fluid. One fluid typically flows through tubes or channels, while the other flows over or through the tubes or channels as shown in figure (I.3). Crossflow heat exchangers offer a balance between the simplicity of parallel flow and the efficiency of counterflow. They are versatile and widely used in various applications.

These flow arrangements have different advantages and are chosen based on factors such as heat transfer requirements, space constraints, and operational considerations. Each arrangement offers unique benefits and trade-offs, and the selection depends on the specific needs of the application, [3].

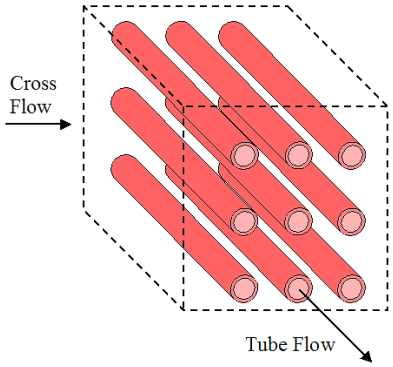

Figure I.3: *Representation of flow direction in a cross-flow heat exchanger*

I.2.4 Classification according to the number of fluids used

The main classifications based on the number of fluids are as follows:

I.2.4.1. Single-fluid heat exchangers

These heat exchangers involve only one fluid in the heat transfer process. The fluid may circulate within a closed system or pass through a heat exchanger to exchange heat with a heated or cooled surface.

I.2.4.2. Two-fluid heat exchangers

These heat exchangers involve two different fluids in the heat transfer process. The two fluids may flow in separate paths inside the heat exchanger, or they may come into direct contact through a heat exchanging surface.

I.2.4.3. Three-fluid heat exchangers

In some cases, heat exchangers may involve three or more fluids in the heat transfer process. These exchangers can be more complex and are often used in specific industrial applications requiring complex thermal flow arrangements.

I.2.5. Classification according to the compactness of the exchanger

Heat exchangers can be classified based on their surface compactness, which refers to the ratio of heat transfer surface area to the volume of the exchanger, as highlights in figure (I.4). This classification helps understand the efficiency and space requirements of different heat exchanger designs. An exchanger is considered compact if its compactness is greater than 700 [m^2/m^3] with the presence of fins, this value may vary from 500 to 800 [m^2/m^3], [4].

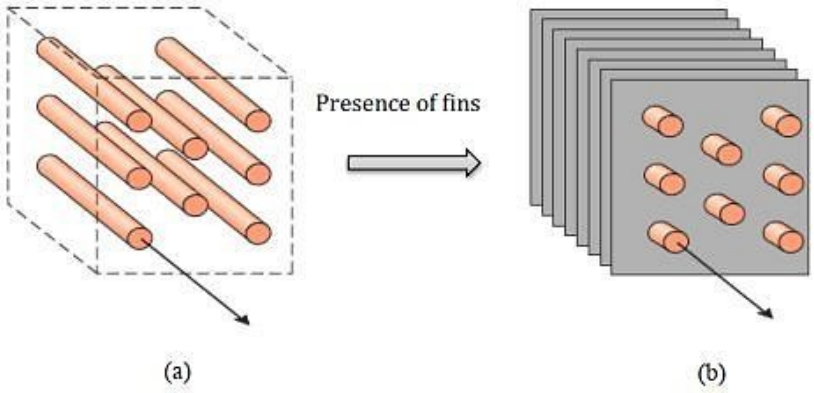

Figure I.4: *(a) heat exchanger without fins, (b) heat exchanger with fins.*

I.3. Heat exchanger types

A heat exchanger is a heat transfer device that exchanges heat between two or more process fluids. Heat exchangers have widespread industrial and domestic applications. Many types of heat exchangers have been developed for use in steam power plants, chemical processing plants, building heat and air conditioning systems, transportation power systems, and refrigeration units. The actual design of heat exchangers is a complicated problem. It involves more than heat-transfer analysis alone. Cost of fabrication and installation, weight, and size play important roles in the selection of the final design from a total cost of ownership point of view. In many cases, although cost is an important consideration, size and footprint often tend to be the dominant factors in choosing a design,[5].

I.3.1. Double-pipe heat exchanger

Consists of two concentric pipes and is perhaps the simplest heat exchanger. This heat exchanger is also suitable where one of both fluids is at very high pressure. Double pipe heat exchangers are generally used for small-capacity application (less than 50 m^2 of total heat transfer surface area). Cleaning is done easily by disassembly as shown in figure (I.5), [6].

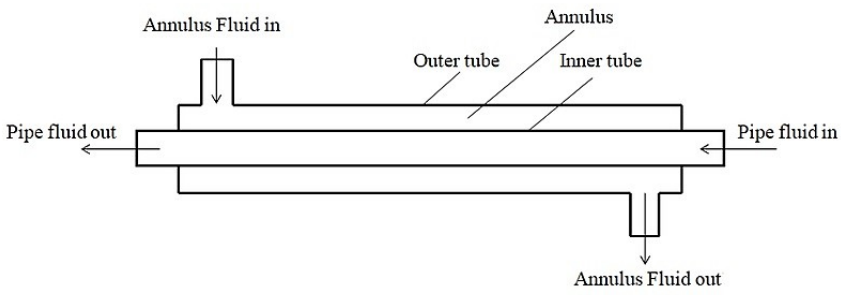

Figure I.5: *schema of double pipe heat exchanger*

I.3.2 Shell-and tube heat exchangers

As illustrated in figure (I.6) Shell-and-tube heat exchangers are commonly used in oil refineries and other large chemical processes. In this model, two separated fluids at different temperatures flow through the heat exchanger, one through the tubes (tube side) and the other through the shell around the tubes (shell side). Several design parameters and operating conditions influence the optimal performance of a shell and tube heat exchanger. This model shows the basic principles of setting up a heat exchanger model. It can serve as a starting point for more sophisticated applications involving parameter studies or additional effects like corrosion, thermal stress, and vibration.

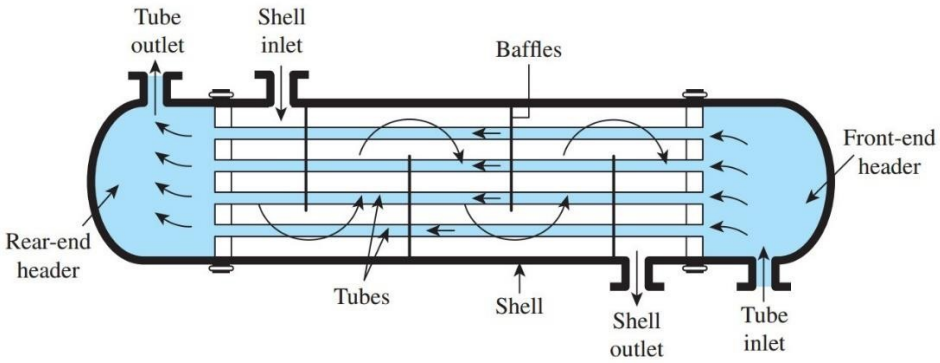

Figure I.6: *shell-and tube heat exchanger.*

I.3.3 Plate Heat Exchanger

Plate heat exchangers are devices used to transfer heat between two fluids. They consist of multiple thin plates arranged in a stack with alternating fluid passages as you can see in figure (I.7). Hot and cold fluids flow through separate channels formed by the gaps between the plates. Heat is transferred from the hotter fluid to the cooler fluid through conduction as they flow in opposite directions and come into close contact with the plate surfaces. Plate heat exchangers offer advantages such as high heat transfer coefficients, efficient thermal performance, compact design, easy maintenance, and flexibility in handling different fluid types and flow rates. They find widespread use in HVAC (Heating, Ventilation, and Air Conditioning) systems, refrigeration systems, chemical processing, food processing, and various other applications requiring efficient heat transfer.

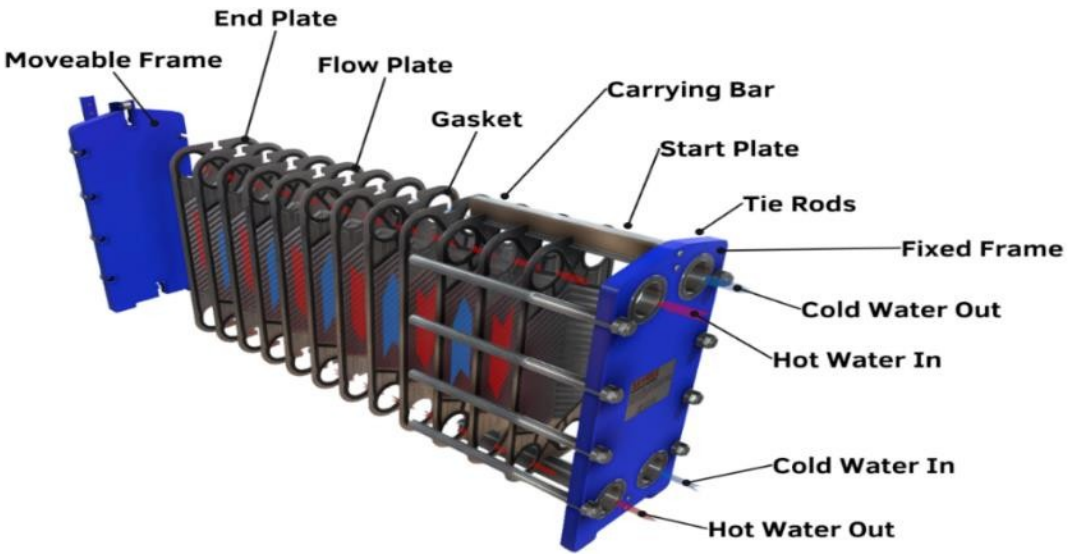

Figure I.7: *Plate Heat Exchanger Components*

I.3.4. Plate fin heat exchanger

This type of heat exchanger uses "sandwiched" passages containing fins to increase the effectiveness of the unit. The designs include cross flow and wavy fins, the compactness factor can be significantly improved (i.e., up to about 6000 (m^2/m^3) by using the plate-fin type of heat exchanger. Figure (I.8) illustrates typical plate-fin configurations. Flat plates separate louvered or corrugated fins, Cross-flow, counter flow, or parallel-flow arrangements can be obtained readily by properly arranging the fins on each side of the plate, [6]. Plate-fin exchangers are generally used for gas-to-gas application, but they are used for low-pressure application not exceeding about 10 atm (that is, 1000kpa). The maximum operating temperatures are limited to about 800 °C. Plate-fin heat exchanger have also been used for cryogenic application, [7].

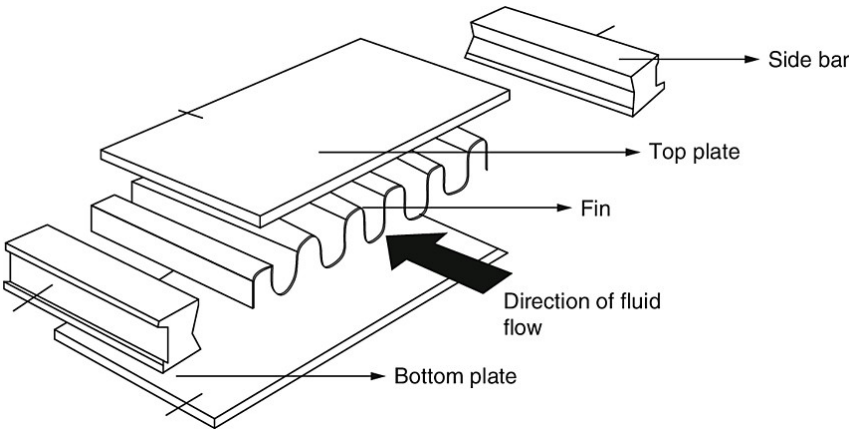

Figure I.8: *plate fin heat exchanger structure.*

I.3.5. Micro channel heat exchangers

Micro channel heat exchangers are multi-pass parallel flow heat exchangers consisting of three main elements: manifolds (inlet end outlet), multi-port tubes with the hydraulic dimeters smaller than 1 mm, and fins as shown in Fig (I.9) all the elements usually brazed together using controllable atmosphere brazing process. Micro channel heat exchangers are characterized by high heat transfer ratio, compact size, and lower airside pressure drop compared to finned tube heat exchanger. Micro channel heat exchangers are widely used in automotive industry as the car radiators, and as condenser, evaporator, and cooling/heating coils in HVAC (Heating Ventilation, And air Conditioning) industry,[7].

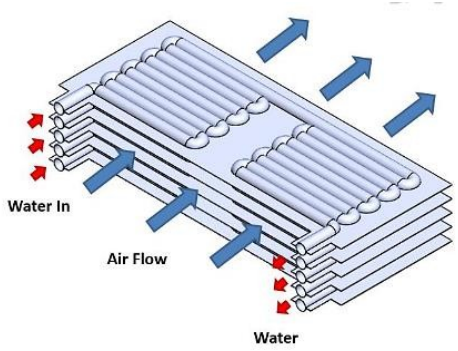

Figure I.9: *Micro channel heat exchangers.*

I.3.6. Helical-coil heat exchangers

Helical-coil heat exchangers are a type of heat exchanger where one or more tubes are wound in a helical (spiral) configuration as shown in figure (I.10). This design allows for a compact and efficient heat transfer process, as the helical shape maximizes the contact area between the fluid flowing through the coil and the surrounding fluid or environment. These heat exchangers are commonly used in applications where space is limited, such as in compact HVAC systems, refrigeration units, and process industries. The helical-coil design enables efficient heat transfer in a relatively small footprint, making it suitable for both heating and cooling applications, [7].

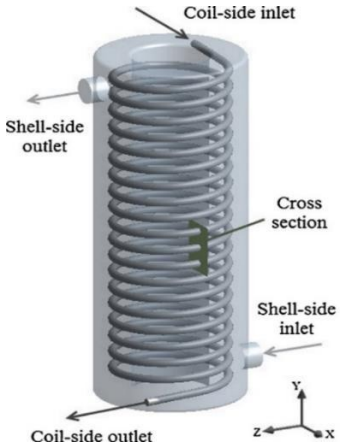

Figure I.10: *schema of shell and helical tube heat exchangers*

I.3.7. Adiabatic wheel heat exchanger

An adiabatic wheel heat exchanger is a specialized type of heat exchanger used primarily in HVAC (Heating, Ventilation, and Air Conditioning) systems for energy recovery purposes, as shown in figure (I.11). It's designed to transfer heat and moisture between two air streams without allowing them to physically mix. This process helps to pre-cool or pre-heat incoming air, depending on the season, thereby improving energy efficiency and reducing the load on heating and cooling systems, [7].

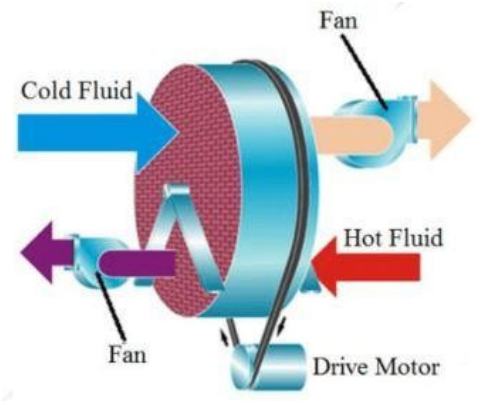

Figure I.11: *Adiabatic wheel heat exchanger.*

I.3.8 Finned-tube heat exchangers

are gas-to-liquid heat exchangers and have dense fins attached on the tube of the air side because the transfer coefficient on the air side is generally one order of magnitude less than that on the liquid side. Circular finned-tube heat exchangers, as shown in figure I.12 (a), are probably well-suited and more practical in large heat exchangers such in air conditioning and refrigerating industries. Flat-finned flat-tube heat exchangers, as shown are mostly used for automotive radiators. The circular finned-tube heat exchangers usually are less compacted than the flat-finned flat-tube heat exchangers, having with a surface area density of about 3300 m^2, [8].

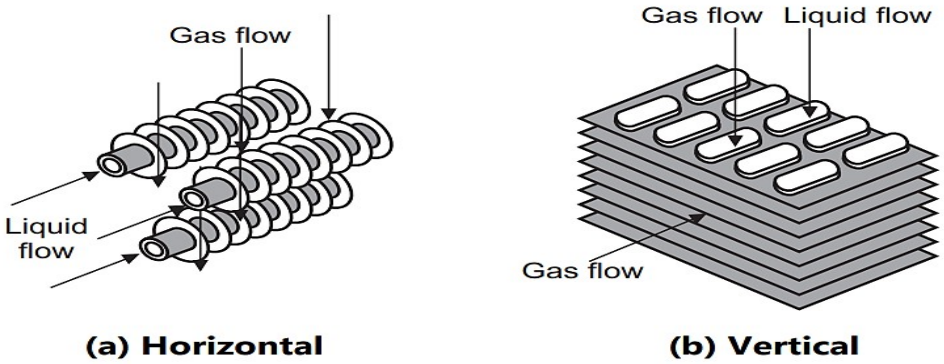

Figure I.12*: typical components of finned-tube heat exchangers, (a) circular finned-tube heat exchanger, (b) Louvered flat-finned flat-tube heat exchanger.*

I.4 Equation and Parameters

I.4.1. Counter flow and parallel Flows

as shown in figure (I.13) two flow configurations (counter-flow and parallel-flow), with temperature distribution for the hot and cold fluids, are considered. The subscripts (i) and (o) indicate inlet and outlet, respectively. The masse flow rate is expressed as $\dot{m}$. [9].

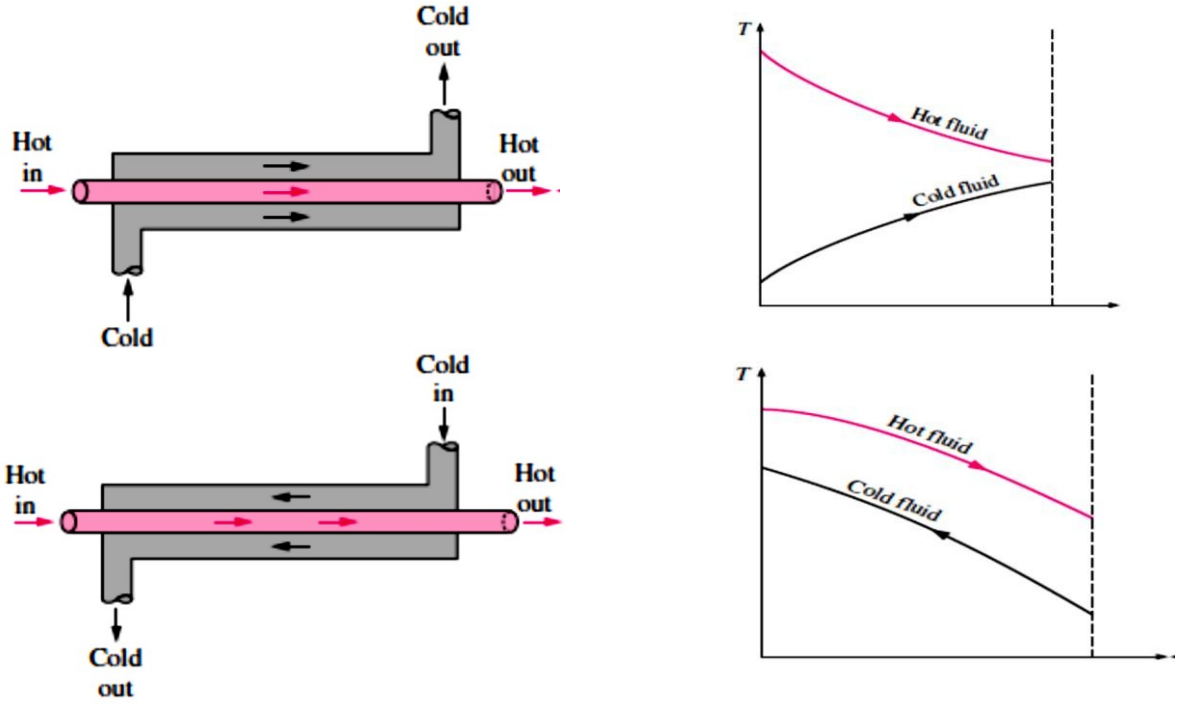

Figure I..13: *schematic channels and temperature distributions for the parallel-flow and counter-flow.*

For the hot fluid, the heat transfer rate is:

$$\boldsymbol{Q = \dot{m}_1\, cp_1(T_{1i} - T_{1o})} \qquad \textbf{(I.1)}$$

Where $\dot{m}$ is the mass flow rate for the hot fluid and cp_1 is the specific heat for the hot fluid for the cold fluid, the same heat transfer is expressed as:

$$\boldsymbol{Q = \dot{m}_2\, cp_2(T_{2i} - T_{2o})} \qquad \textbf{(I.2)}$$

Where $\dot{m}_2$ is the mass flow rate for the hot fluid and cp_2 is the specific heat for the cold fluid the same heat transfer rate can be expressed in terms of the overall heat transfer coefficient

$$\boldsymbol{Q = UAF\Delta T_{1m}} \qquad \textbf{(I.3)}$$

Where U is the overall heat transfer coefficient and a is the heat transfer surface area at the hot or cold side. F is the correction factor, depending on the flow arrangements. For example, F=1 for counter flow arrangements,[10].

Note that:

$$\boldsymbol{UA = U_1 A_1 = U_2 A_2 = UA_1 = UA_2} \quad \textbf{(I.4)}$$

And ΔT_{1m} is the log mean temperature difference that as:

$$\boldsymbol{\Delta T_{lm} = \frac{\Delta T_1 - \Delta T_2}{ln(\frac{\Delta T_1}{\Delta T_2})}} \quad \textbf{(I.5)}$$

Where:

$$\boldsymbol{\Delta T_1 = T_{1i} - T_{2i}} \quad \text{and} \quad \boldsymbol{\Delta T_2 = T_{1o} - T_{2o}} \quad \text{for parallel flow} \quad \textbf{(I.6)}$$

$$\boldsymbol{\Delta T_1 = T_{1i} - T_{2o}} \quad \text{and} \quad \boldsymbol{\Delta T_2 = T_{1o} - T_{2i}} \quad \text{for counter flow} \quad \textbf{(I.7)}$$

Equation (I.1) (I.2) and (I.3) are the basic equation for counter flow and parallel flow heat exchangers. Hence, any combinations of three unknowns among all parameter ($T_1, T_2, A_0 and\ q$)

Can be solved where the heat transfer area is:

$$\boldsymbol{A_1 = P_1 L} \quad \textbf{(I.8-a)}$$

Or

$$\boldsymbol{A_2 = P_2 L} \quad \textbf{(I.8-b)}$$

Where $P_1\ and\ P_2$ are perimeter of hot and cold fluid channels, respectively.

I.4.2. Overall Heat Transfer Coefficient

Construction a thermal circuit across a wall between hot and cold fluids as shown in figure (I.14) the temperature different ($T_{1i} - T_{2i}$) seems complex varying along the length L, which can be represented by the log mean temperature different ΔT_{lm} , [11].

$$\boldsymbol{q = \frac{T_{1i} - T_{1o} - T_{2i} - T_{2o}}{\frac{1}{UA}} = \frac{F\Delta_{lm}}{\frac{1}{h_1 A_1} + R_w + \frac{1}{h_2 A_2}}} \quad \textbf{(I.9)}$$

Where h_1 and h_2 are the heat transfer coefficients for hot and cold fluids, Respectively, and A_1 And A_2 are heat transfer surface areas for hot and cold fluids, respectively and R_w is the wall thermal resistance [10].

the wall thermal resistance is:

$$\boldsymbol{R_{w} = \frac{\delta_w}{k_w A_w}} \quad \textbf{(I.10)}$$

Where δ_w is the thickness of the flat wall and k_w is the thermal conductivity of the wall and A_w is the heat transfer area of the wall, which is the same as A_1 or A_2 in this case, [11].

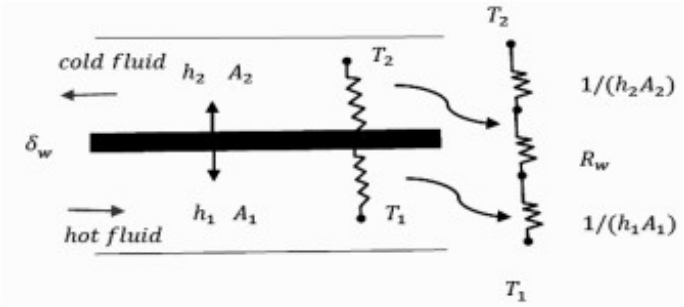

***Figure I.14**: thermal resistance and thermal circuit for a heat exchanger for flat walls*

For concentric tubes (double-pipe heat exchanger), the wall thermal resistance is:

$$R_w = \frac{ln(\frac{d_0}{d_i})}{2\pi R_w L} \quad \textbf{(I.11)}$$

Where d_i and d_o are the inner and outer diameter of the circular wall and L is the tube length the overall heat transfer coefficient for the cold fluid with the heat transfer area A_2 is:

$$U_2 = \frac{\frac{1}{A_2}}{\frac{d_0}{h_i A_1} + R_w + \frac{1}{h_2 A_2}} \quad \textbf{(I.12)}$$

For a double-pipe heat exchanger (Concentric pipes) with neglecting the wall conduction we have:

$$U_0 = \frac{1}{\frac{d_0}{h_i A d_i} + \frac{1}{h_o}} \quad \textbf{(I.12a)}$$

F: is the correction factor, which is determined by the heat exchanger's shape as well as the temperatures of the hot and cold fluid flows at the intake and output.

$$F = \frac{\frac{\sqrt{R^2+1}}{R-1} Ln\left(\frac{1-P}{1-PR}\right)}{Ln\left(\frac{(2/P)-1-R+\sqrt{R^2+1}}{(2/P)-1-R-\sqrt{R^2+1}}\right)} \quad \textbf{(I.13)}$$

You can obtain correction factor from the charts as illustrated in figure (I.15) based on two parameters, P and R. Such that:

$$\begin{cases} P = \frac{t_2 - t_1}{T_1 - t_1} \\ R = \frac{T_2 - T_1}{t_2 - t_1} \end{cases} \quad \textbf{(I.14)}$$

where:

- t_1 and t_2 – Inlet and outlet temperature for shell side of the heat exchanger.
- T_1 and T_2 – Inlet and outlet temperature for tube side of the heat exchanger.

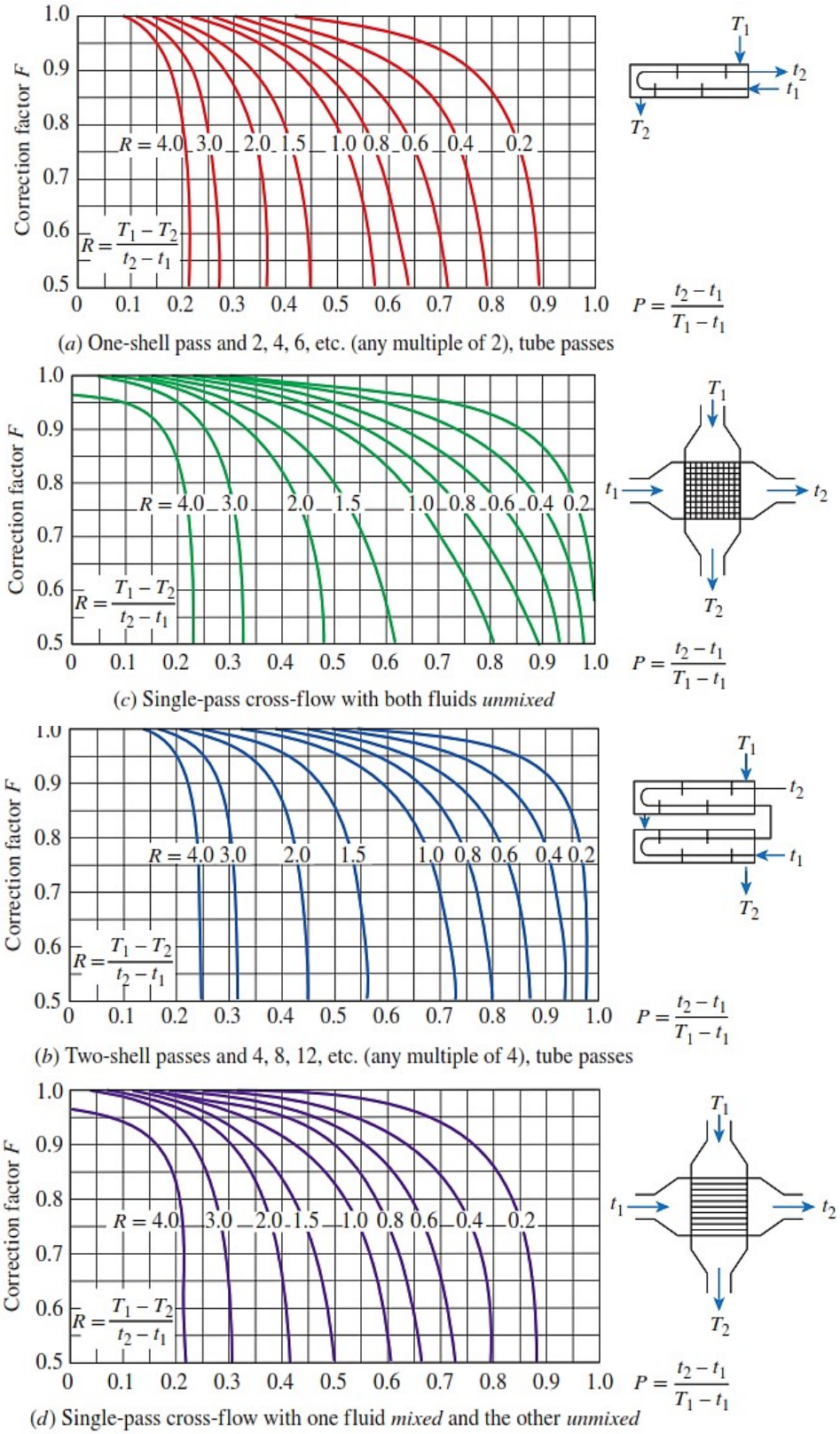

Figure I.15: *Correction factor F charts for common shell-and-tube and crossflow heat exchangers. Source: Bowman, Mueller, and Nagle, 1940.*

I.4.3. Nusselt numbers in Tubular Flow

An empirical correlation was developed by seeder and Tate to predict the mean Nusselt number for laminar flow in a circular duct for the combined entry length with constant wall temperature, [12].

The average Nusselt number is a form of:

$$\boldsymbol{Nu_d = \frac{hD_e}{k_f} = 1.86\left(\frac{D_h R_e P_r}{L}\right)^{\frac{1}{3}}\left(\frac{\mu}{\mu_s}\right)} \quad \textbf{(I.15)}$$

$0.48 < pr < 16.7$

$0.0044 < \left(\frac{\mu}{\mu_s}\right) < 9.75$

use $Nu_D = 3.66$ if $Nu_D < 3.66$

All the properties are evaluated at the mean temperature $T_{1m} = \frac{T_{1i}+T_{10}}{2}$ for a hot fluid or

$T_{2m=}\frac{T_{2i}+T_{20}}{2}$ For a cold fluid except μ_s that is evaluated at the wall surface temperature.

Gilinsky recommended the following correlation valid over a large Reynolds number range including the transition region, [8]. The number is:

$$\boldsymbol{NU_D = \frac{hD_e}{k_f} = \frac{\left(\frac{f}{2}\right)(Re_{D-1000})Pr}{1+12{,}7\left(\frac{f}{2}\right)^{\frac{1}{2}}\left(pr^{\frac{2}{3}}-1\right)}} \quad \textbf{(I.16)}$$

$3000 < Re_D < 5 * 10^6$

$0.5 \leq pr \leq 2000$

Where the friction factor f is obtained assuming that the surface is smooth as:

$$\boldsymbol{f = (1.58\ln(Re_D) - 3.28)^{-2}} \quad \textbf{(I.17)}$$

I.4.4. Effective-NTU (ε-NTU) Method

When the heat transfer rate is not known or the outlet temperatures are not knowing tedious iterations with the LMTD method are required. In an attempt to eliminate the iterations, kays and London in 1955 developed a new method called the effective-NTU method. Which is a widely used approach for analyzing heat exchangers and estimating their thermal performance. NTU stands for Number of Transfer Units, while ε represents the effectiveness of the heat exchange, current practice tends to favor the effectiveness approach because both effectiveness and the number of transfer units have a unique physical significance for a given exchanger and given flow thermal capacities, [9].

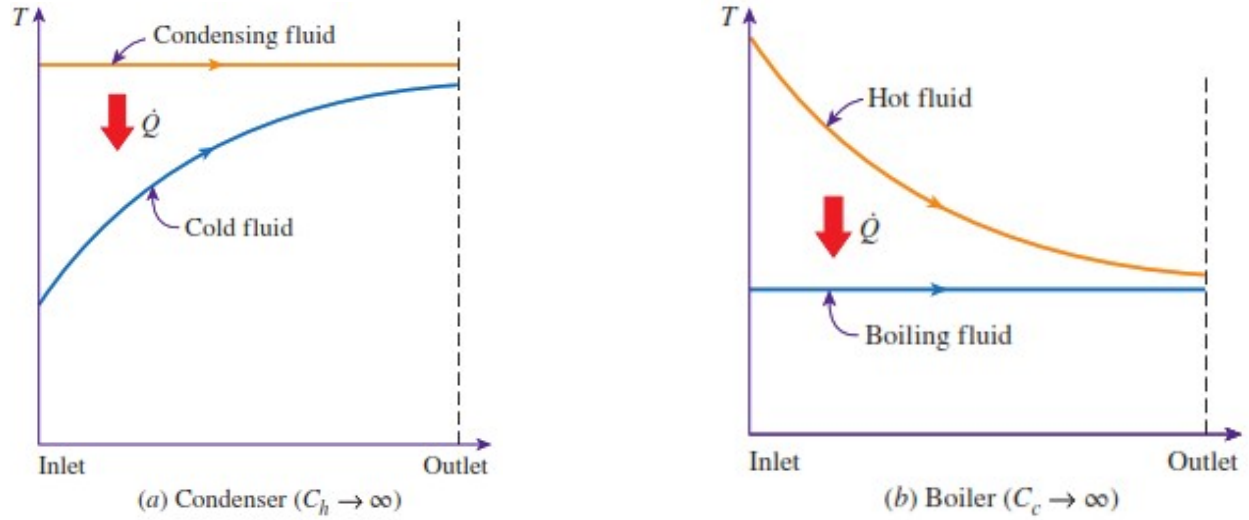

Figure I.16: *Maximum possible heat transfer rate, (a) when* $\dot{m}_2 cp_2 < \dot{m}_1 cp_1$ (b) $\dot{m}_2 cp_2 > \dot{m}_1 cp_1$

Heat capacity rate is the product of mass flow rate and specific heat ($c_1 = \dot{m}_1\, cp_1$) the minimum capacity rate is defined as the one that a lesser capacity rate. The maximum capacity rate is then the one that has a higher capacity rate. As shown in both Fig (I.16) (a) and (b), the minimum capacity curve always approaches the maximum capacity curve because the lower capacity fluid experiences more quickly thermal exchanger (gain or lose thermal energy) compared to the high-capacity fluid. considering both the maximum temperature difference ($T_{1i} - T_{2i}$) and the minimum heat capacity as an approaching medium, [12].

The maximum possible heat transfer rate can be formulated as:

$$\boldsymbol{q = (\dot{m}cp)_{min}(T_{1i} - T_{2i})} \qquad \textbf{(I.18)}$$

The heat exchanger effectiveness ε is then written by

$$\boldsymbol{\varepsilon = \frac{Actual\ Heat\ Tansfer\ Rate}{Maximum\ pssible\ Heat\ Tansfer\ Rate} = \frac{Q}{Q_{max}}} \qquad \textbf{(I.19)}$$

The heat transfer unit (NTU) is defined:

$$\textbf{NTU} = \boldsymbol{\frac{UA}{(\dot{m}\, cp)_{min}}} \qquad \textbf{(I.20)}$$

The heat capacity ratio C_r is defined:

$$\boldsymbol{C_r = \frac{(\dot{m}cp)_{min}}{(\dot{m}cp)_{max}}} \qquad \textbf{(I.21)}$$

I.4.4.1. parallel-flow

Consider a parallel-flow heat exchanger for which $(\dot{m}_2 cp_2 > \dot{m}_1 cp_1)$ or equivalently $[(\dot{m}\, cp)_{min} = \dot{m}_1 cp_1]$ from equation (I.19) with equation (I.20) and (I.21), we obtain:

$$\boldsymbol{C_r = \frac{(\dot{m}cp)_{min}}{(\dot{m}cp)_{max}} = \frac{(T_{20}-T_{2i})}{(T_{1i}-T_{1o})}} \quad \textbf{(I.22)}$$

From equation (I.5) with equation (I.1) and (I.2), we can express:

$$\boldsymbol{\varepsilon = \frac{q}{q_{max}} = \frac{(\dot{m}_1 cp_1)(T_{1i}-T_{1o})}{(\dot{m}cp)_{min}(T_{1i}-T_{2i})} = \frac{(\dot{m}_2 cp_2)(T_{2i}-T_{2o})}{(\dot{m}cp)_{min}(T_{1i}-T_{2i})}} \quad \textbf{(I.23)}$$

$$\boldsymbol{\varepsilon = \frac{q}{q_{max}} = \frac{(T_{2i}-T_{2o})}{(T_{1i}-T_{2i})}} \quad \textbf{(I.24)}$$

The heat exchanger effectiveness ε for parallel flow is obtained:

$$\boldsymbol{\varepsilon = \frac{1-exp\,[-NTU(1+C_r)]}{1+C_r}} \quad \textbf{(I.25)}$$

Where NTU and C_r are referred to equation (I.18) and (I.19)

Solving for NTU for parallel flow, we have:

$$\textbf{NTU=-}\boldsymbol{\frac{1}{1+C_r}\ln\,[1-\varepsilon(1+C_r)]} \quad \textbf{(I.26)}$$

Since the same result is obtained for $\dot{m}_2 cp_2 < \dot{m}_1 cp_1$ or equivalently $(\dot{m}cp)_{min} = \dot{m}_2 cp_2$, equation (I.22) applies for any case of parallel-flow heat exchanger

I.4.4.2. Counter flow

Based on a completely analogous analysis, the heat effectiveness for counter flow is obtained as:

$$\boldsymbol{\varepsilon = \frac{1-\exp\,[-NTU(1-C_r)]}{1+C_r\exp\,[-NTU(1-C_r)]}} \quad \textbf{(I.27)}$$

Solving for NTU for counter flow, we have:

$$\boldsymbol{NTU = \frac{1}{1-C_r}\ln\left(\frac{1-\varepsilon C_r}{1-\varepsilon}\right)} \quad \textbf{(I.28)}$$

Using equation (I.27) and (I.26), the actual heat transfer rate is expressed in terms of the effectiveness, inlet temperatures and a minimum heat capacity rate.

TABLE I.1: Type of heat exchanger and the relation of effectiveness. *NTU=UA/C_{min} and c=C_{min}/C_{max} =$(\dot{m}c_p)_{min}$ =$(\dot{m}c_p)_{max}$*

Heat exchanger type	Effectiveness Relation
1- Double pipe:	
Parallel flow	$\varepsilon = \frac{1-exp\,[-NTU(1+C)]}{1+C}$
Counterflow	$\varepsilon = \frac{1-exp[-NTU(1-C)]}{1-C\,exp[-NTU(1-C)]}$
2- shell-and-tube	
One-shell pass 2, 4... Tube Passes	$\varepsilon_1 = 2\{1+c+\sqrt{1+c^2}\,\frac{1+exp[-NTU_1\sqrt{1+c^2}]}{1+exp[-NTU_1\sqrt{1+c^2}]}\}$
n-shell passes 2n,4n.... tube passes	$\varepsilon = [(\frac{1-\varepsilon_1 c}{1-\varepsilon_1})^{n} - 1]\,[(\frac{1-\varepsilon_1 c}{1-\varepsilon_1}) - c]^{-1}$
3 - Crossflow (single-pass)	
both fluids Unmixed:	$\varepsilon = 1 - \exp\{\frac{NTU^{0.22}}{C}[\exp(-cNTU^{0.78}) - 1]\}$
C_{max} **mixed,** C_{min} **unmixed**	$\varepsilon = \frac{1}{c}(1 - \exp\{-c[1 - \exp(-NTU)]\}$
C_{min} **mixed** C_{max} **unmixed**	$\varepsilon = 1 - exp\{-\frac{1}{c}[1 - exp(-cNTU)]\}$
4- All heat exchangers	
If c=0	$\varepsilon = 1 - \exp(-NTU)$

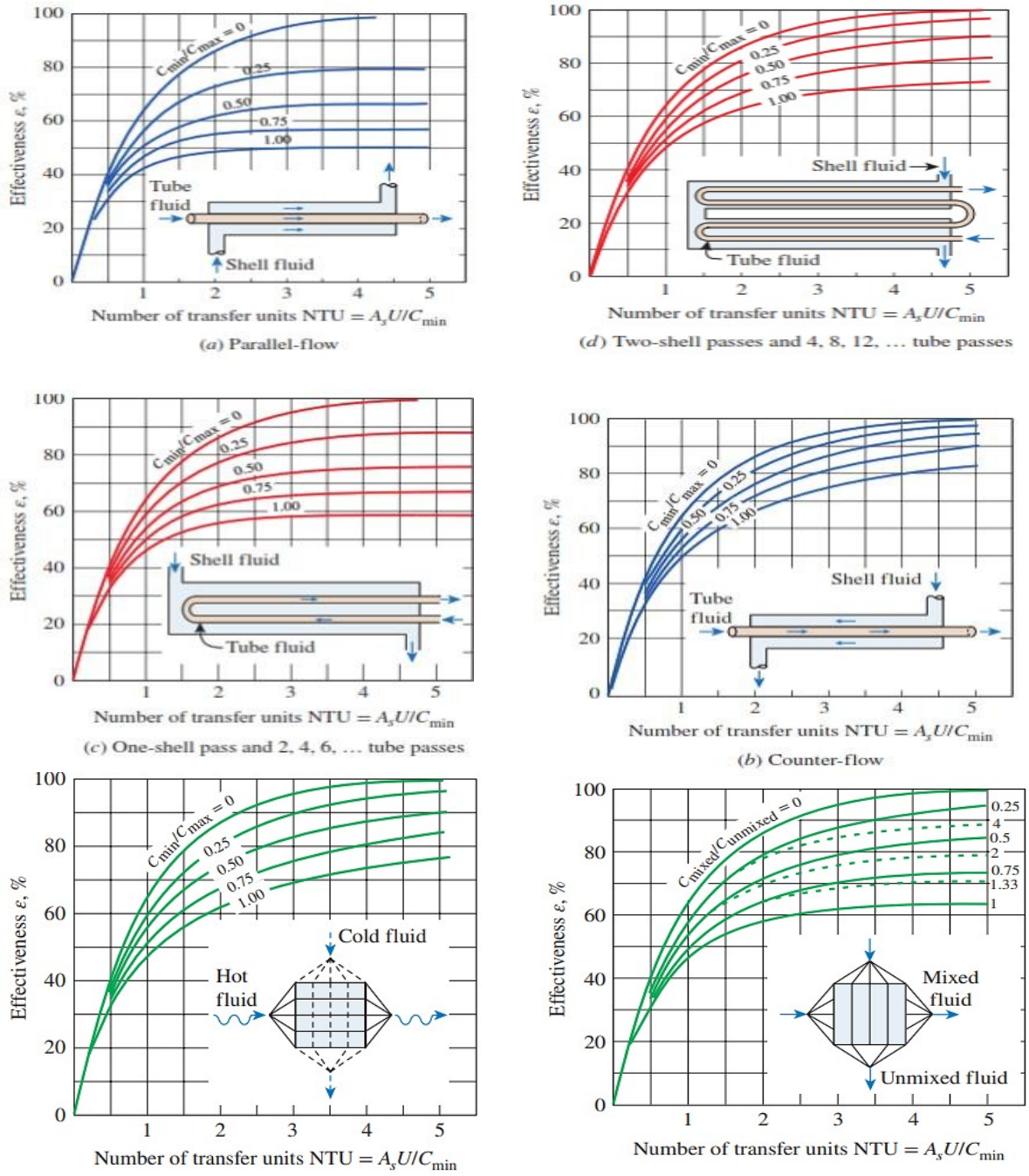

Figure I.17: *Effectiveness unit in terms of number of transfers in heat exchangers.*

REFERENCES:

[1] Ramesh k. shah and Dusan P. sekulic fundamentals of heat exchanger design. 1 copyright 2003 Jonhn wiley & sonc, Inc

[2] ELLABED Nadia, Etude de dimensionnement d'un échangeur de chaleur dans unmilieu cryogénique, Magister Ecole Nationale Polytechnique d'Oran, optimisation dessystèmes énergétiques (2012).

[3] F. Mebarek Oudina. Échangeurs de chaleur. Cours et exercices corrigés. Livre, édition Al-Djazair, université 20 Aout 1955 Skikda (2014)

[4] TAOURIT Farida, Étude du comportement dynamique et thermique de deuxécoulements du fluidedans un échangeur de chaleur (comparaison entre le cas simple et lecas avec ailettes), Master université Abou Bakr Belkaid-TLEMCEN-Energétique (2013).

[5] B. Zohuri compact heat exchangers Springer International publishing Switzerland 2017.

[6] hosung lee compact hrat Exchangers chapter5

[7] sunders, E.A. (1988). Heat Exchanges: selection, Desing and construction. New York: Longman scientific and technical.

[8] hosung lee compact hrat Exchangers chapter5

[9] sidic kakac and hongtan liu heat exchangers selection, rating, and thermal designe

[10] Foumeny, E.A., and P.J. Heggs. 1991. Heat exchanger engineering, volume 2,

compact heat exchangers: Techniques of size reduction. West Sussex, England: Ellis

Horwood Limited

[11] kays, W.M., and AL. London. 1964. Compact heat exchangers, 2nd ed. New York: McGraw Hiil

[12] Boyen, J.L.1975.practical heat recovery. New YORK: John Wiley & Sons

Chapter 02

PROBLEM AT HAND

Introduction:

This chapter is dedicated to describing the different steps adopted in our work to achieve the geometry building in terms of different steps carried out to create the whole crossflow heat exchanger design composed by shell and the tube bundle with two distinguish arrangement configurations: In-line and staggered, as highlighted in Figure (II.1).

The second part provides the illustrative details of the mesh used for calculation, including all the functions and modifications carried out on the mesh in terms of sizes and treatment of boundary layers (inflation option) in order to capture all relevant physical properties involved for the numerical model.

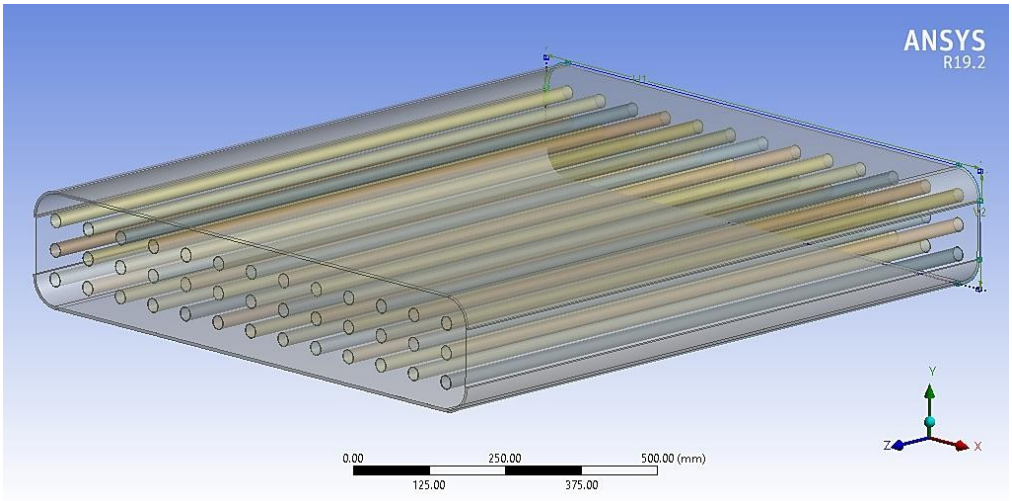

Figure.II.1. *cross-flow type heat exchanger.*

The last part will focus on defining the CFD problem and setting it up with appropriate initial and boundary conditions. Indeed, in this section, it is important to specify the solver settings to obtain accurate results. In this chapter also, we will present the different choice suitable to numerically investigate the CFD problem of cross-flow heat exchanger to demonstrate how to set up the solver and show iterative schemes using various options available in the Solution tab of Ansys Fluent.

1. Geometry:

To build the geometry used in our study, we first use the software design modeler integrated into the ANSYS workbench. The heat exchanger's geometry is constructed of parallel straight tubes with 39 passageways that are encircled by a shell. The copper tubes have a diameter of

24 mm and a thickness of 1mm, while the steel shell measures (1200x1000x200 mm^3). with thickness of 5mm, during that process, we took several stages, which we'll go over in detail below.

- We changed the measurement unit from meter to millimeter.
- We started by sketching shell in the (x, y) coordinate system by drawing the shape of it with 1000 mm length and 200 mm width see figure (II.2).

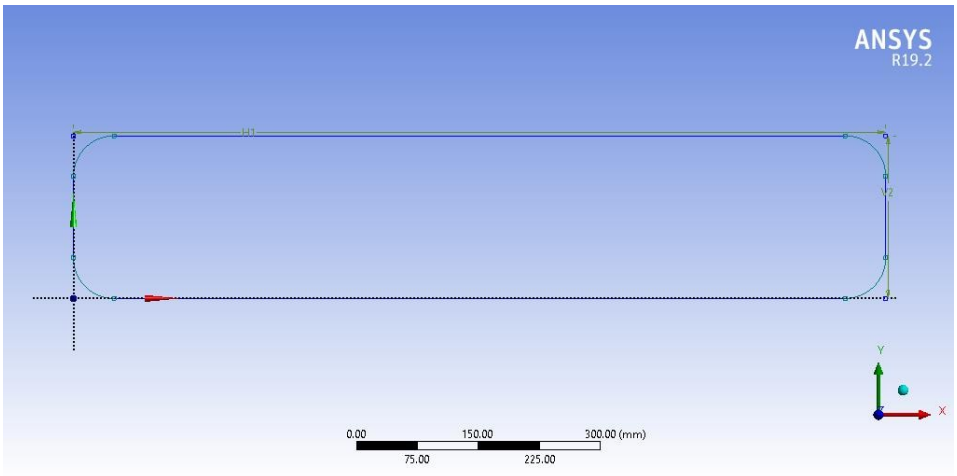

Figure II.2. The shell shapes.

- And then we extruded the pre-draw shell and set the depth to 1200mm, with a thickness of 5 mm and then we generate the desired shape see figure (II.3).

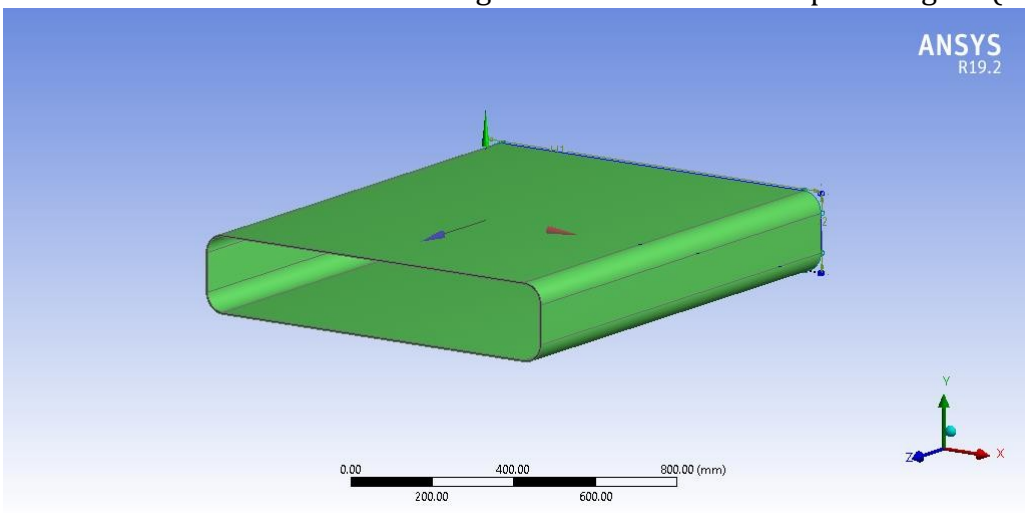

Figure. II.3. The extruder procedure.

- And then we created a new "xy" coordinate system and we draw two rectangles connected to the shell with 5 mm width and 10 cm length shown in figure (II.4).

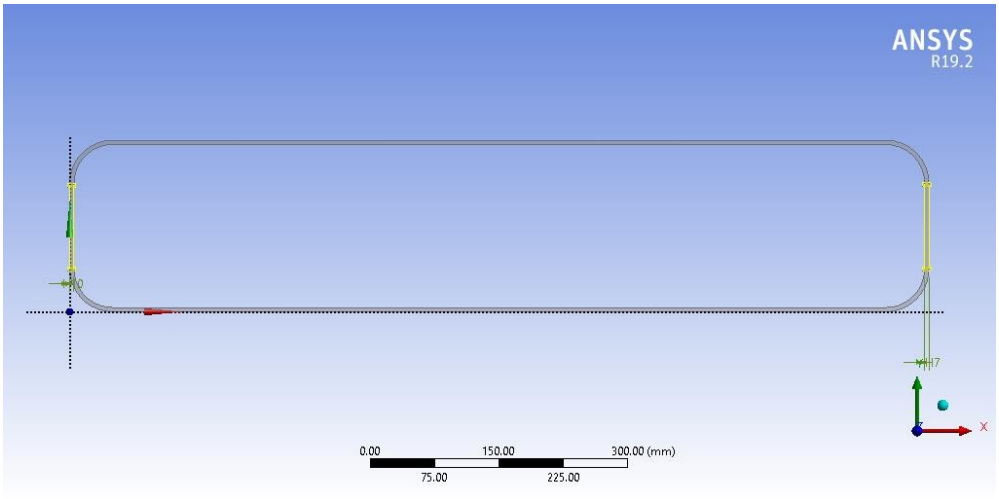

Figure. II.4. the shell sides.

- And then we extruded the pre-draw rectangular and set the depth to 1200mm as apparent in figure (II.5).

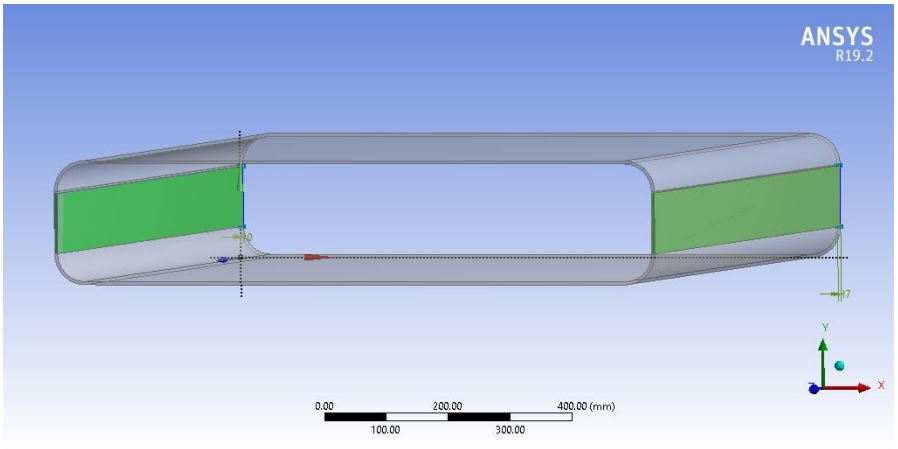

Figure. II.5. The extruder procedure.

Following the completion of the tube drawings, we were thorough in tracing the steps required to build the appropriate tubes for our heat exchanger, which are listed below in stages.

- To begin, we created a new "xy" coordinate system and we draw the cylinder with diameter of 24 mm and thickness of 1 mm as Observed in figure (II.6).

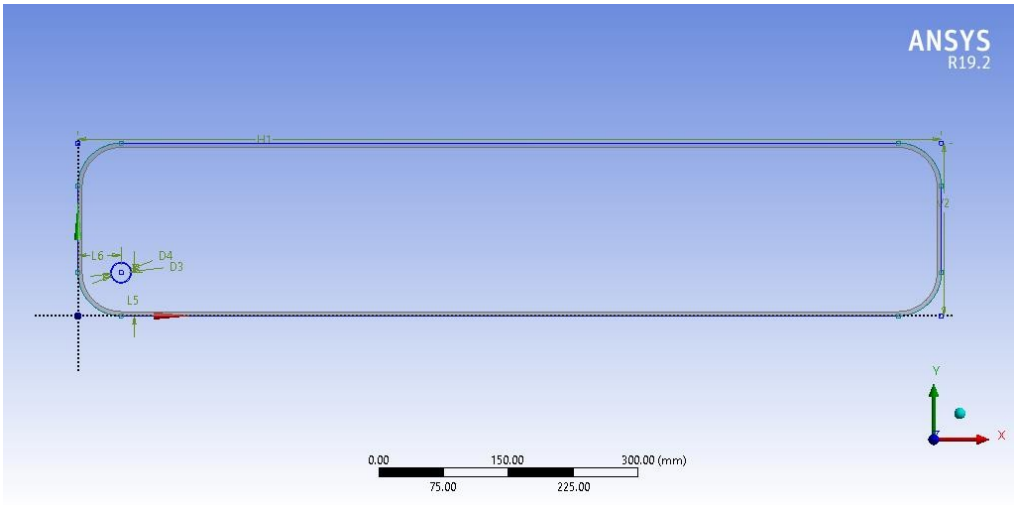

Figure. II.6. the tube shapes.

- After setting the depth to 1200mm and extruding the pre-drawn cylinder, we produced a complete three-dimensional tube as appears in figure (II.7).

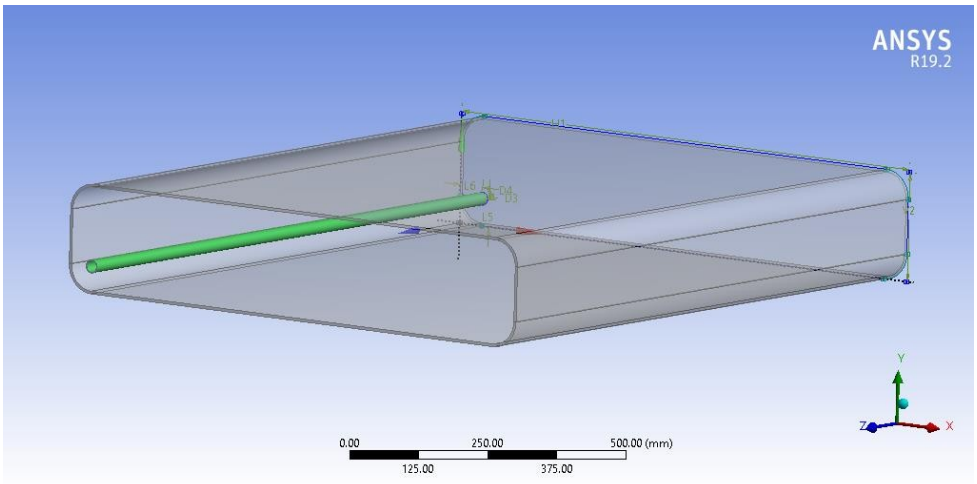

Figure. II.7. Extrude procedure.

- we use the filling tool by selected the internal face of the tube to ensure that it was filled to our specifications so the hot fluid entrance and exit outside the tube as observed in figure (II.8).

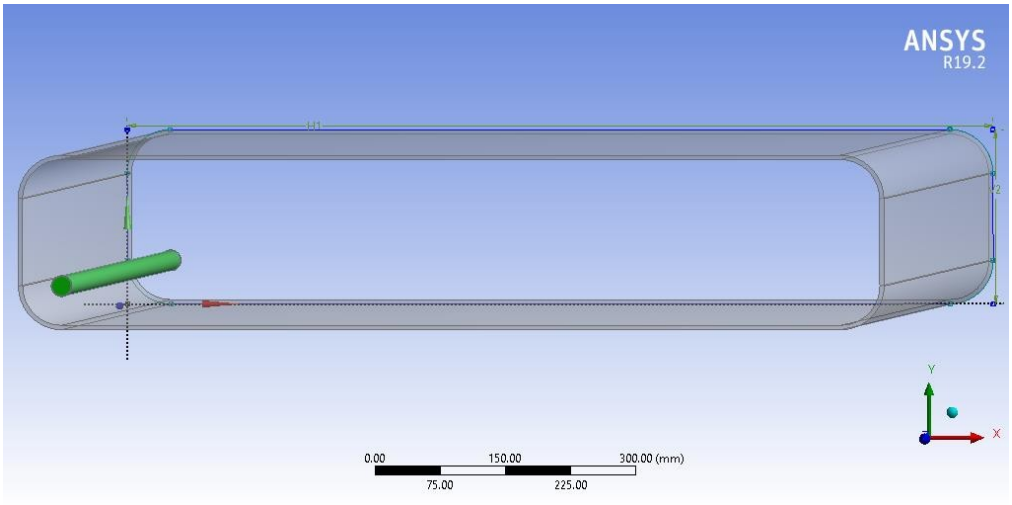

Figure. II.8. The filling procedure of the tube.

- then when we finished the fill process, first we used the patterns feature to duplicate the cylinder in the X direction by selecting the tube, second, we select all the tubes and duplicate them again in the Y direction as can be seen in figure (II.9).

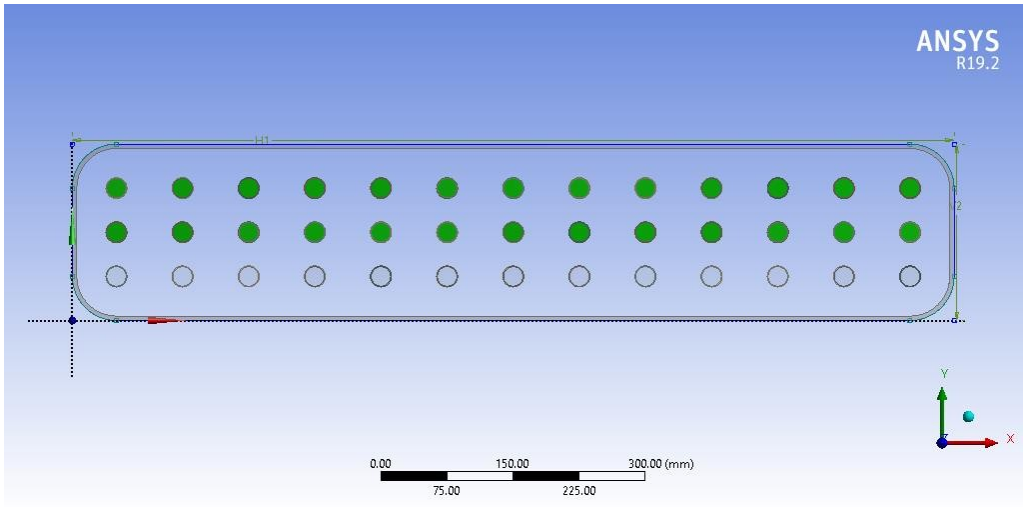

Figure. II.9. The patterns procedure.

- All what was left is to fill the shell domain and this is through selected the internal face of the shell to ensure that it was filled to our specifications reflected in figure (II.10).

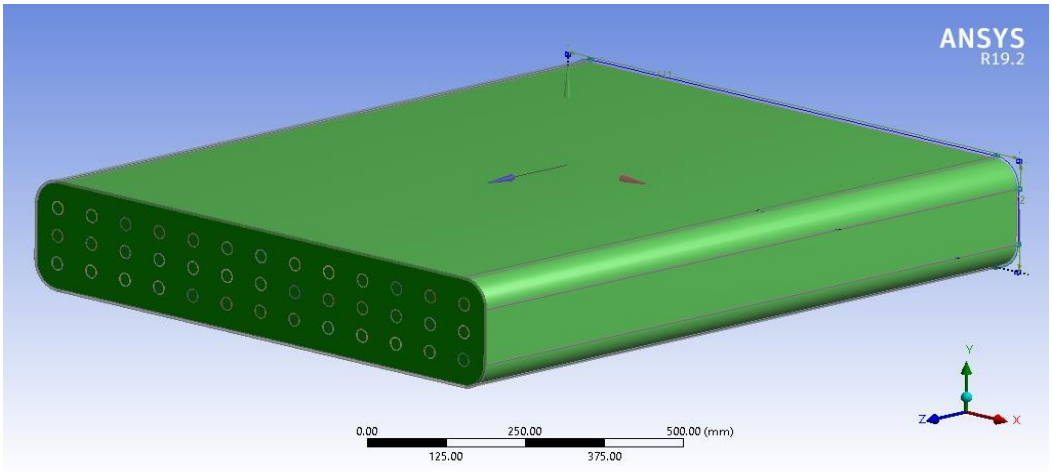

Figure. II.10. The filling procedure of the shell.

- we used the subtract option to build a Boolean and choose the form to be separated (the cold liquid) from (shell + tube + hot fluid) see figure (II.11).

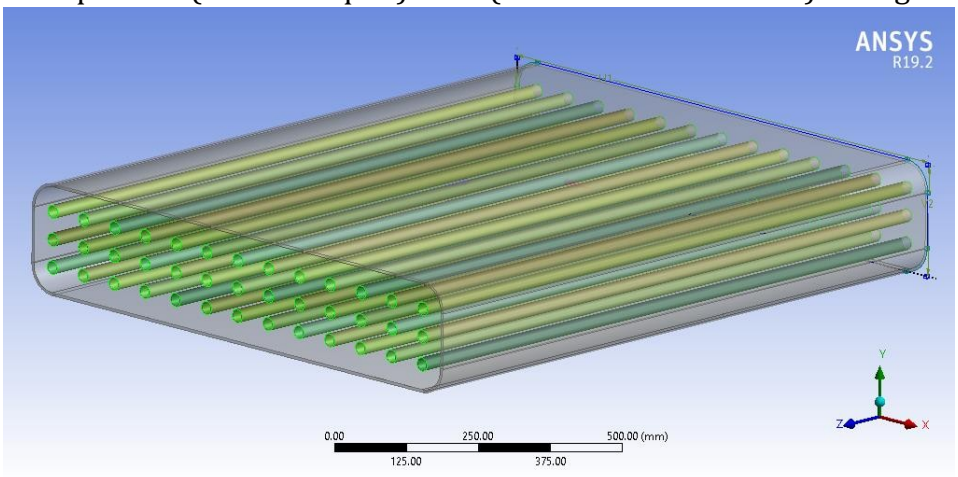

Figure. II.11. The Boolean procedure.

- and to separate the left and right side from the shell so that we make the entrance and the exit of the cold fluid, The shapes were approved to be kept, and we were left with the final shape of the heat exchanger as illustrated in figure (II.12).

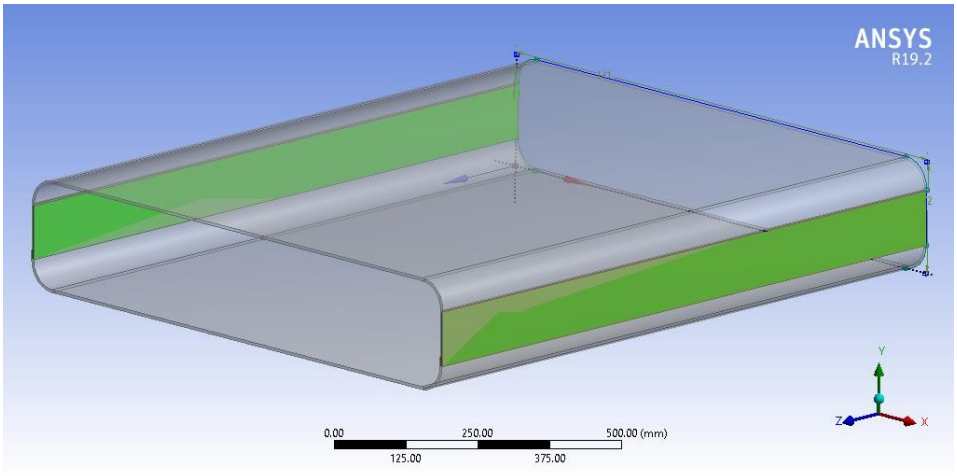

Figure. II.12. The Boolean procedure.

Finally, as depicted in Figure (II.13) the last heat exchanger arrived, bringing the geometry phase with all of its peculiarities to a close.

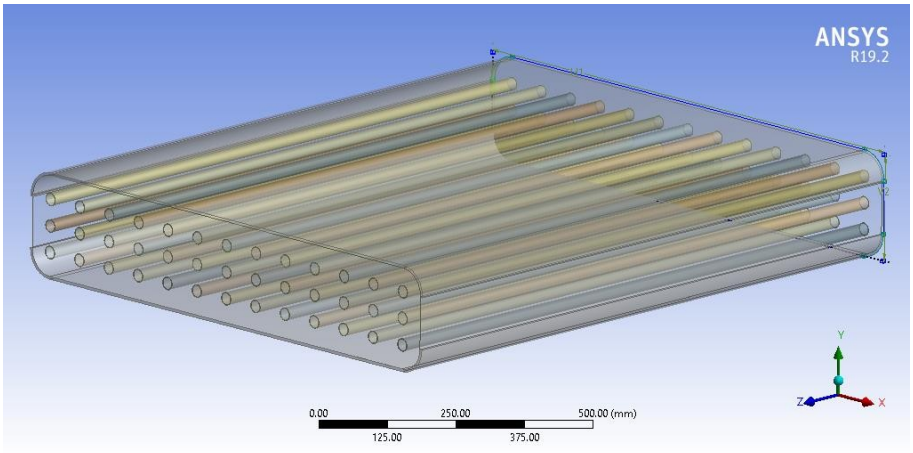

Figure. II.13. final structure (cross-flow type heat exchanger).

2. Mesh:

For the purpose of numerical analysis, meshing is the act of dividing a complicated form into more manageable, smaller pieces, or "mesh." As it directly affects the quality and dependability of the findings, this phase is crucial in Ansys R19.2.

Later on, the first work to be accomplished in carrying out a numerical simulation is the definition of a mesh adapted to the nature of the flow. To execute the simulation, an

appropriate calculation mesh is necessary. Several mesh densities were tested to have the appropriate mesh that ensures the best possible calculation accuracy and conforms to the complicated geometry of the shape as shown in figure (II.14). It was generated by a workstation that has a 32-core CPU and 128GB of RAM. This mesh contains mixed cells (Tetra and Hexahedral cells) having both triangular and quadrilateral faces at the boundaries. The consecutive results are considered as a criterion for choosing the mesh of the structure. The size of elements and the number of nodes has also been explored, as illustrated in table (II.1).

2.1 Mesh size:

Eléments	Node	Corps	Minimum élément size
10825600	10939681	81	3 mm

Table.II.1. heat exchanger statistics.

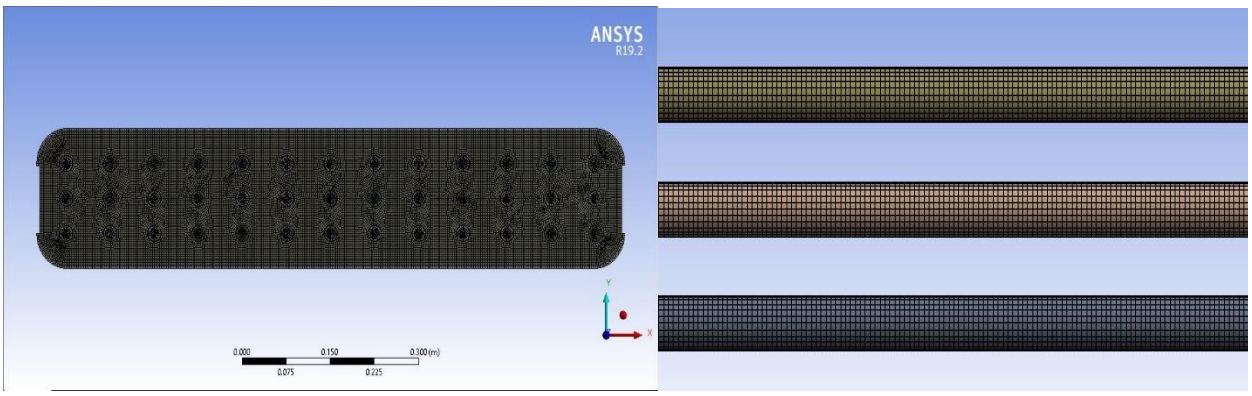

(a) (b)

Figure.II.14. (a) the final refined mesh, (b) hexahedral mesh of the tube part

3. Set up:

Upon importing the geometry and mesh file into the ANSYS FLUENT software, the solver type "Pressure-Based" is chosen, signifying an incompressible flow. Subsequently, the selection of a steady-state regime which mean it's not related to the time.

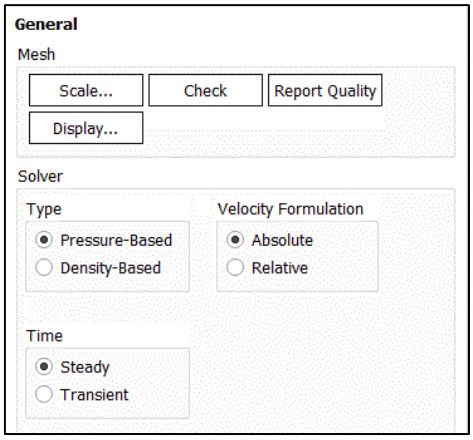

Figure.II.15. Selection of the steady-state regime for an incompressible flow.

3.1. Activation of the energy equation:

Enabling the energy equation is necessary in order to take the thermal impact into account when addressing the problem under study.

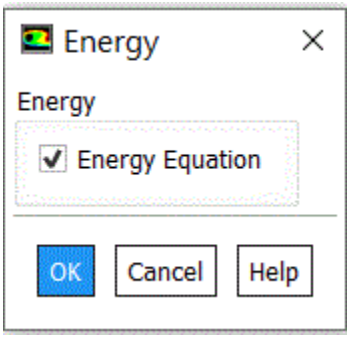

Figure.II.16. Activation of the energy equation.

3.2. Definition of the turbulence model:

The "Standard k-epsilon" turbulence model under the "viscous Model" tab is chosen in order to take turbulence in the researched problem into consideration.

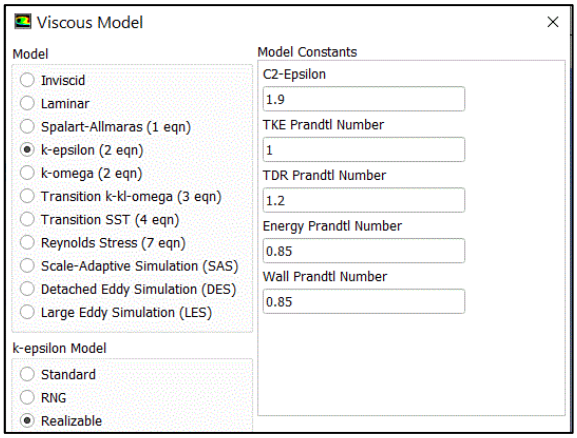

Figure.II.17. Selection of the Standard k-epsilon turbulence model.

3.3. Set up of materials used:

Materials	Density (kg⁄m3)	Specific heat (J/kg. °C)	Thermal conductivity(W⁄m.°C)	Viscosity (Pa. S)
Liquid water	998.1	4181	0.6	0.001003
Oil	710	3300	0.22	0.01
Steel	8030	501.48	16.17	
Copper	8978	381	387.6	

Table.II.2. Properties of all materials used.

3.4. Set up the cell zone conditions:

For solid materials we had chosen copper for the inner pipes and steel for the outer shell, and as for liquid materials, we had chosen hot oil passes inside the tubes and the cold water in the shell domain for two configurations of tubes arrangement (In-line-Staggered) and depending on the subject of our study, we have two different cases that we study and compare:

- First case: Laminar flow for both configurations.
- Second case: Turbulent flow for both configurations.

3.5. Set up the boundary conditions:

	Case I		Case II	
	Hot fluid (Oil)	Cold fluid (Water)	Hot fluid (Oil)	Cold fluid (Water)
	Inlet	Inlet	Inlet	Inlet
Temperature	200°C	15°C	200 °C	15 °C
Velocity	1 cm/s	0.5 cm/s	20 cm/s	10 cm/s

Table.II.3. Boundary conditions for the four cases studied.

3.6. The convergence monitor:

For every transport equation, we selected a convergence monitor of order (0^{-6}) By selecting the "Residual Monitors" option.

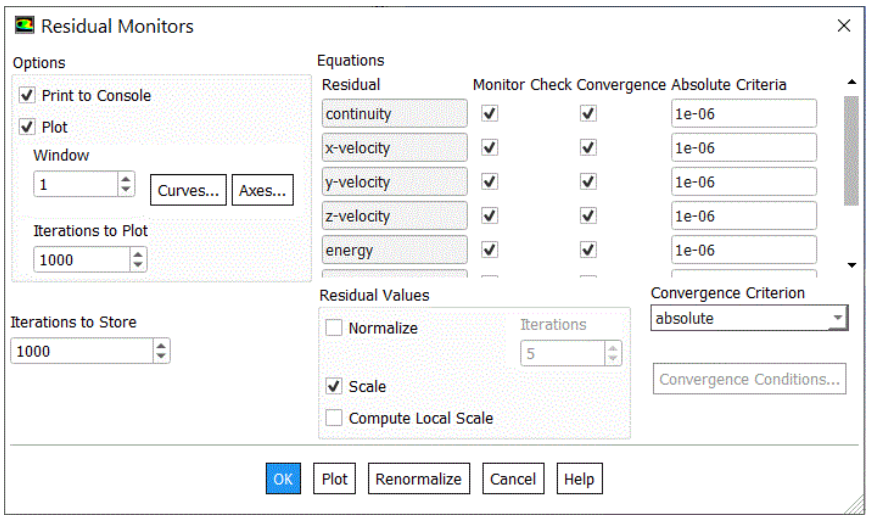

Figure.II.18. The convergence monitors.

3.7. Initialization of solutions:

Before starting the calculation, in this study standard initialization has been chosen which typically refers to set initial values for variables like velocity, pressure, and temperature before starting the simulation.

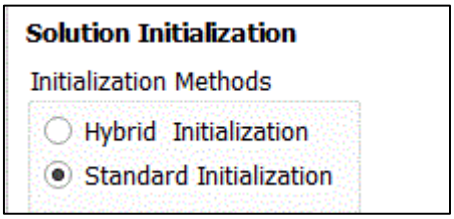

Figure.II.19. Initialization of solutions.

3.8. Launching the calculation:

Finally, after all the steps are completed, we entered 1000 iterations to make sure during the calculation, the software iteratively refines the solution until it reaches convergence, meaning that the solution stabilizes within an acceptable accuracy.

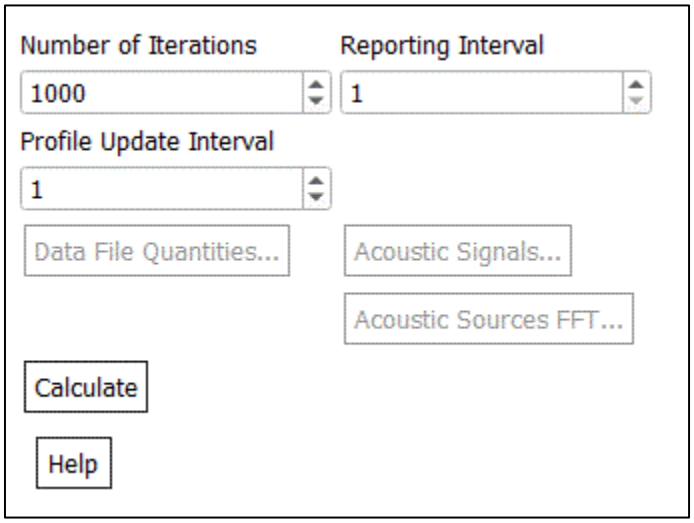

Figure.II.20. Launching the calculation.

4. Mathematical formulation:

In a turbulent heat exchanger simulation using ANSYS Fluent, the software solves a set of governing equations to model the behavior of fluid flow and heat transfer. Some of the equations including:

4.1. Continuity Equation (Mass Conservation):

The continuity equation represents the conservation of mass and states that mass cannot be created or destroyed in an isolated system. The total mass of the system remains constant over time, regardless of the processes happening within the system, [1].

The continuity equation in a steady regime and for an incompressible fluid is given by:

$$\nabla V = 0 \qquad \textbf{(II.1)}$$

Where:

- $\nabla.V$ represents the divergence of the velocity vector V.

4.2. Momentum Equation:

The momentum equation is a fundamental principle in fluid dynamics that describes the motion of fluid particles in response to external forces. It is derived from Newton's second law of motion and is a key equation used to analyze and predict fluid flow behavior. If the force acting on a body is known as a function of time, also the velocity and position of the body as functions of time can, theoretically, be derived from Newton's equation by a process known as integration.

The general form of the momentum equation for fluid flow can be expressed as, [1]:

$$\rho \frac{Du}{Dt} = -\frac{\partial P}{\partial x} + div(\mu grad\, u) + S_{Mx} \quad \textbf{(II.2)}$$

$$\rho \frac{Dv}{Dt} = -\frac{\partial P}{\partial y} + div(\mu grad\, v) + S_{My} \quad \textbf{(II.3)}$$

$$\rho \frac{Dw}{Dt} = -\frac{\partial P}{\partial z} + div(\mu grad\, w) + S_{Mw} \quad \textbf{(II.4)}$$

4.3. The *k-epsilon* model:

The K-epsilon (*k-ε*) turbulence model is a frequently utilized model in computational fluid dynamics (CFD) for simulating mean flow characteristics under turbulent flow conditions. It is a two-equation model that uses two transport equations (also known as partial differential equations) to describe turbulence in general. The first transported variable is turbulent kinetic energy, k. The second transported variable in this case is the turbulent dissipation, epsilon. It is the variable that determines the scale of the turbulence, whereas the first variable, k, determines the energy in the turbulence, [1]. The basic equations for the k-epsilon model are:

Transport equation for turbulent kinetic energy k:

$$\frac{\partial(\rho K)}{\partial t} + \nabla(\rho k U) = \nabla.\left[(\mu + \frac{\mu_t}{\sigma_k})\nabla K\right] + P_k - \varepsilon \quad \textbf{(II.5)}$$

Transport equation for the rate of dissipation of turbulent kinetic energy epsilon:

$$\frac{\partial(\rho \varepsilon)}{\partial t} + \nabla(\rho \varepsilon U) = \nabla.\left[(\mu + \frac{\mu_t}{\sigma_\varepsilon})\nabla \varepsilon\right] + C\varepsilon_1 P_k - C\epsilon_1 \frac{\varepsilon}{K} \quad \textbf{(II.6)}$$

where:

- ρ = the density of the fluid
- v = the velocity vector of the fluid
- μ is the dynamic viscosity of the fluid

- μ_t = the turbulent viscosity, which is modeled using the turbulent kinetic energy and the rate of dissipation of turbulent kinetic energy
- σ_k and σ_ε = the model constants
- P_k = the production of turbulent kinetic energy due to mean velocity gradients
- ε = the rate of dissipation of turbulent kinetic energy due to viscous effects
- $C_{\varepsilon 1}$ and $C_{\varepsilon 1}$ = model constants.

Therefore, the *K*-ε model is well-known and often used in industry and This model is valid in turbulent areas. It has been designed historically for free flows, i.e., plane jets and mixing layers (Launder & Spalding), [2].

Chapter 03

RESULTS AND DISCUSSIONS

Preamble

In this chapter the different numerical results obtained from the full 3D model dealing with the four different cases of cross heat exchanger configurations will be discussed and compared. These cases include two heat transfer fluids: water and oil flowing in two distinguished configurations: in-line and staggered with different inlet boundary conditions in terms of velocity and temperature. A second parametric study constituting of increasing the velocity twenty times for both configurations, was also examined. The main goals of this numerical analysis are to evaluate the global heat transfer characteristics of each type of heat exchanger in terms of evolution in both temperature field, dynamic field, and finally the thermal efficiency.The results are presented and compared through visualizations, including contours, charts, and streamlines. The study attempts to determine the most appropriate heat transfer properties for real-world applications by looking and analyzing these data. The analysis takes into account a number of performance measures, including the total heat transfer rate and the heat transfer coefficients.

III.1. Discussion of the results

As well-known, heat exchangers usually operate for long periods of time with no change in their operating conditions. Therefore, they can be modeled as steady-flow devices. As such, the mass flow rate of each fluid remains constant, and the fluid properties such as temperature and velocity at any inlet or outlet remain the same. Also, the fluid streams experience little to no change in their velocities and elevations, and thus the kinetic and potential energy changes are negligible. The specific heat of a fluid, in general, changes with temperature. But in a specified temperature range, it can be treated as a constant at some average value with little loss in accuracy. Axial heat conduction along the tube is usually insignificant and can be considered negligible. Finally, the outer surface of the heat exchanger is assumed to be perfectly insulated, so that there is no heat loss to the surrounding medium, and any heat transfer occurs between the two fluids only. The idealizations stated above are closely approximated in practice, and they greatly simplify the analysis of a heat exchanger with little sacrifice in accuracy. Therefore, they are commonly used.

Under these assumptions, the first law of thermodynamics requires that the rate of heat transfer from the hot fluid be equal to the rate of heat transfer to the cold one. That is:

$$\boldsymbol{Q = \dot{m}_c Cp_c (T_{c,out} - T_{c,in}) = \dot{m}_h Cp_h (T_{h,in} - T_{h,out})} \quad \textbf{(III.1)}$$

Where:

the subscripts "*c*" and "*h*" stand for cold and hot fluids, respectively and;

- m_c, m_h = mass flow rates
- Cp_c, Cp_h = specific heats
- $T_{c,out}$, $T_{h,out}$ = outlet temperatures
- $T_{h,in}$, $T_{c,in}$ = inlet temperatures

The heat transfer rate Q is taken to be a positive quantity, and its direction is understood to be from the hot fluid to the cold one in accordance with the second law of thermodynamics.

Moreover, in order to examine the effect of the flow regime of the cold fluid (water) in the shell, i.e. laminar and turbulent on the efficiency of the resulting heat transfer of the different configurations, the inlet velocity was increased twenty times with maintaining the same thermal boundary conditions, as illustrated in the table (III.1):

Table.III.1. *Boundary conditions for the four cases studied.*

	Case I		**Case II**	
	Hot fluid (Oil)	Cold fluid (Water)	Hot fluid (Oil)	Cold fluid (Water)
	Inlet	Inlet	Inlet	Inlet
Temperature	200°C	15°C	200 °C	15 °C
Velocity	1 cm/s	0.5 cm/s	20 cm/s	10 cm/s

III.1.1 Temperature evolution

After obtaining the numerical results of the four cases of single-pass cross-flow heat exchangers with cold fluid (water) mixed and the hot one (oil) unmixed, a temperature contours was plotted to further examine their evolution of both coolants hot and cold. The results give quantitative and qualitative details indicating the evolution of the temperature field for all cases. These results will be used in the next sections to calculate the overall heat transfer coefficient as well as the efficiency of each heat exchanger configuration in order to identify the most efficient in terms of thermal performance.

The analysis of temperature fields for all cases cited previously of the heat exchangers types, are presented in Figure (III.1). In order to illustrate the thermal behavior of the two heat transfer fluids for each case, the temperature fields of the pipe walls are exported and graphically presented in terms of isotherm contours. For this purpose, two planes are chosen: horizontal (*XZ*) at hallway-up and vertical (*XY*) at mid-width (see Figure III.1).

As expected, for both cases a significant decrease in the temperature of the hot fluid, and against an increase in the cold fluid temperature, are clearly observed. Obviously, in all case this exit of the cold fluid never exceeds the outlet temperature of the hot fluid as well known in the case of the double-pipe heat exchanger with counterflow configuration. The temperature of the hot fluid, which enters the tube at 473K, decreases gradually as it flows through the tube until it reaches the outlet. Similarly, the temperature of the cold fluid, which enters the shell at a temperature of 288K, increases gradually as it flows through the shell until it reaches the outlet. The calculation results give that in the case I, corresponding to the laminar flow in the shell, the average temperatures of the cold fluid (water) at the shell outlet, for the in-line and staggered arrangements, are 311.7K and 310.9K, respectively. However, the temperature of the hot fluid outlet at the exit of the pipes is almost 339.8K, for the in-line arrangement and 342.2K for the staggered arrangement.

Arrangement	Case I (laminar flow)	Case II (turbulent flow)
In-line	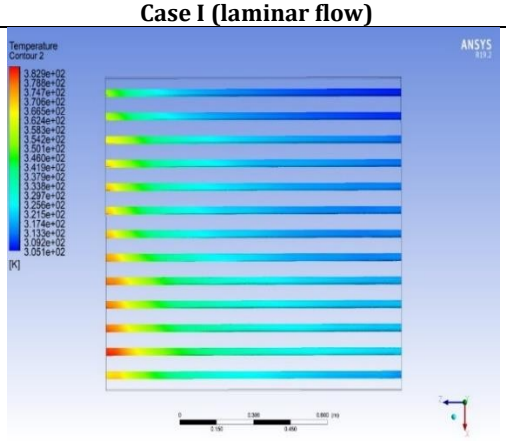	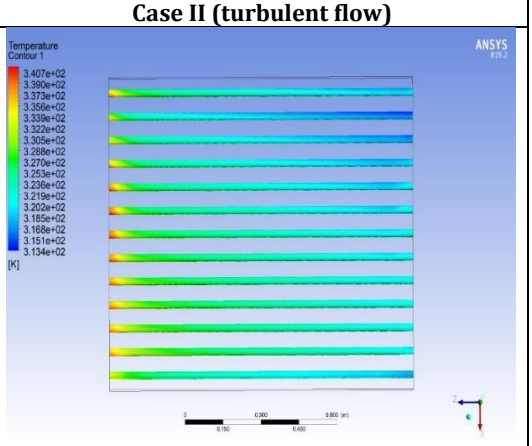
	Horizontal planes (XZ) selected at hallway-up	
	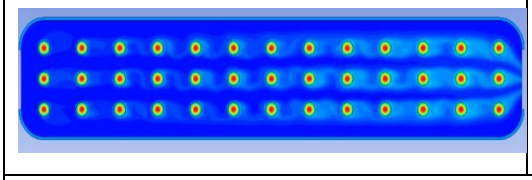	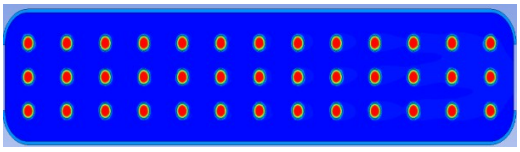
	Vertical planes (XY) selected at mid-width	
Staggered	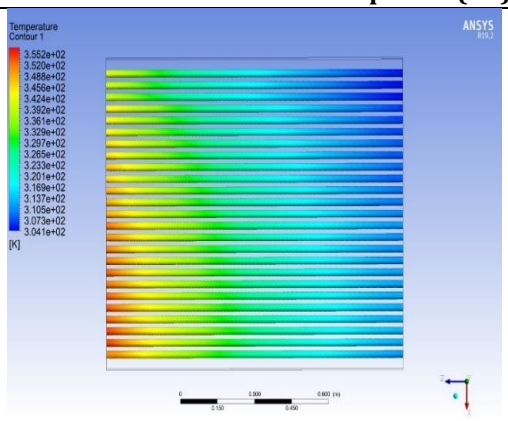	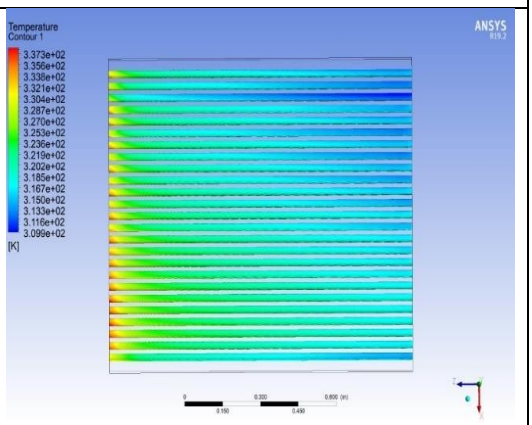
	Horizontal planes (XZ) selected at hallway-up	
	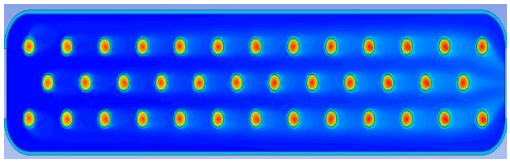	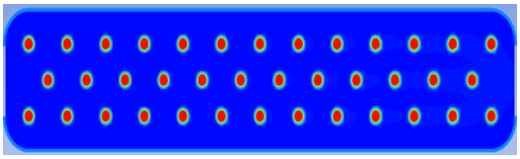
	Vertical planes (XY) selected at mid-width	

Figure.III.1: *Temperature evolution in pipe walls of both cases for the different arrangements.*

Similarly, in the case II, corresponding to the turbulent flow, the temperatures of the cold fluid (water) at the shell outlet, for the in-line and staggered arrangements, are 299K and

298K, respectively. However, the temperature of the hot fluid outlet at the exit of the pipes is almost 431K, for the in-line arrangement and 435K for the staggered arrangement.

III.1.2. Charts analyses:

In light of the above analysis performed on the of the maps of temperature contours using the color legend, it's clear that the temperatures gradually changed, fluctuated, and finally settled at the tube's exit. This fluctuation made it challenging to understand the heat exchange taking place in and around the tube. Hence, to further understand the thermal process, other graphical options were explored. Indeed, charts were created in order to follow the evolution of the temperature through a straight line connecting three selected positions inside the bank of tubes (purple, pink, light blue) parallel to the pipe-wall for the cold fluid, and the same goes for the evolution of the temperature of the hot fluid by choosing (blue, red, green) goes through the pipe walls (see the following figure).

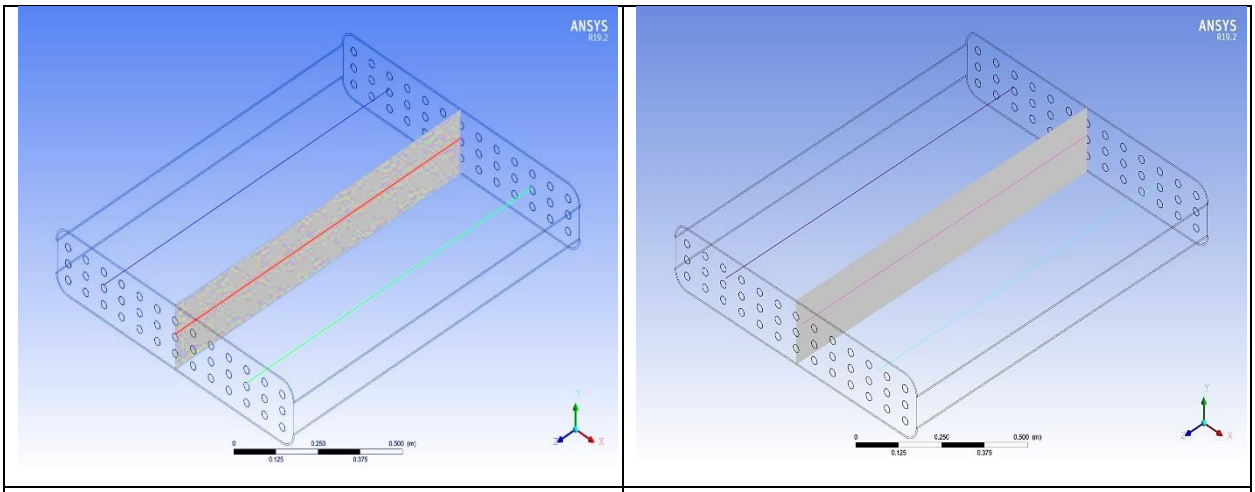

(a) straight lines selected for the hot fluid | *(b) straight lines selected for the cold fluid*

Figure III.2: *Technique for monitoring the evolution of temperature for the two heat transfer fluids: (a) blue, red, green line for hot fluid goes through the pipe walls and, (b) purple, pink, light blue line parallel to the pipe for the cold fluid.*

Figure (III.3) summarizes the results obtained through the chosen exploration lines in terms of temperature evolution for the two heat transfer fluids cold and hot corresponding to the two chosen configurations, i.e. in-line and staggered. Figure (III.3-a) corresponding to the case I, clearly shows that the temperature of pipe walls starts from 382K and steadily decreases until it reaches the end of the pipes at 310K, while the cold fluid (water) begins at temperature of 305K fluctuates while its rising to 360K near the end of pipes. However, for the case II sketched in Figure (III.3-b) the temperature of pipe walls starts from 337K and then decreases according to the length of the pipe until it reaches 317K. Also, the cold fluid (water) begins at 300K and increase until achieves 315K at the end.

Arrangement	Case I (laminar flow)	Case II (turbulent flow)
in-line	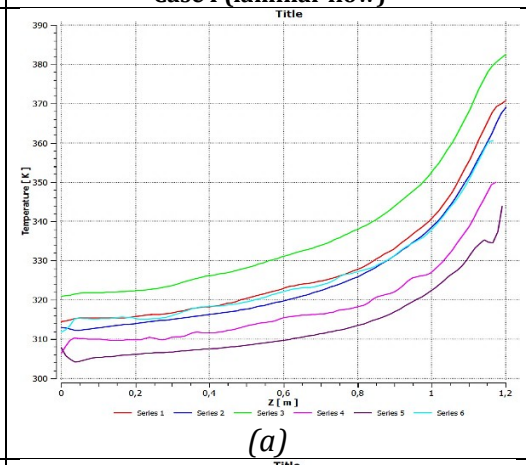 *(a)*	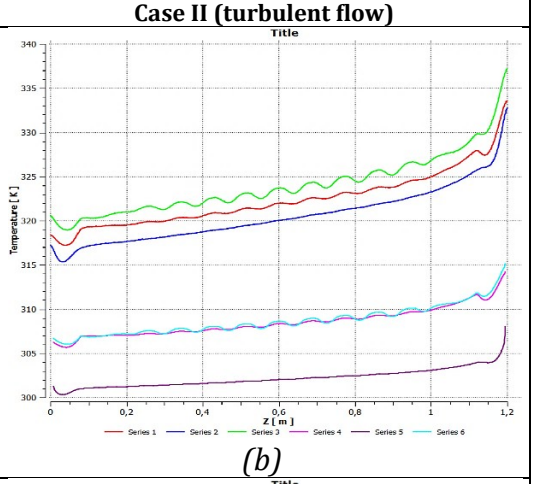 *(b)*
Staggered	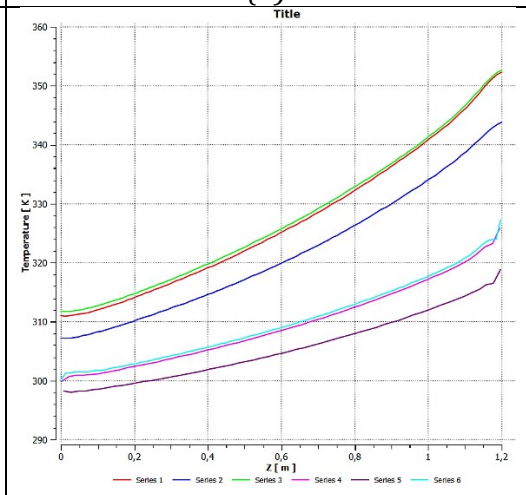 *(c)*	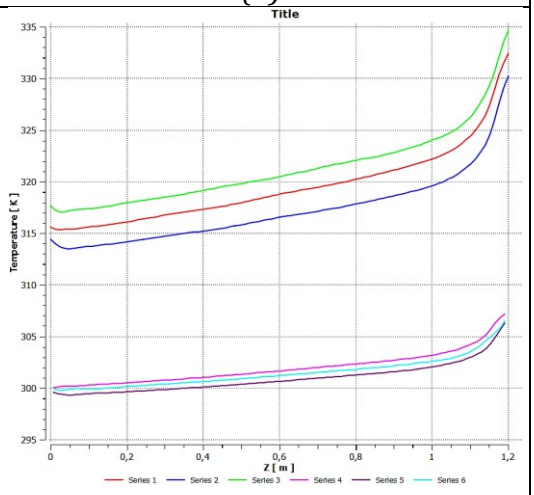 *(d)*

Figure III.3: *Temperature evolution of both heat transfer of the cold fluid and pipe walls for the in-line and staggered configurations*

While for the case of staggered arrangement, the temperature of the contact interface between the hot fluid (Oil) and the pipes-walls start form 354K in case I (laminar flow presented in Figure III.3-c) and 335K for the case II related to the turbulent flow as it is illustrated in Figure (III.3-d), decreasing according to the selected length of the pipes which subsequently exchange the heat flux with the cold fluid (water) which enters with a fixed temperature equal to 300K in both cases and begins to increase until its reach a level.

Moreover, the comparative study performed on these results clearly indicated that the nature of the flow regime significantly affected the heat exchange in all cases in terms of efficiency. Indeed, the case I (laminar flow in shell), the in-line configuration gives that the temperature difference is $\Delta T = 72K$. By contrast, in the case II this difference does not exceeds 25K. The same goes for the cold fluid was observed, where the temperature differences for the case I and II for the in-line arrangement, are 55K and 15K, respectively.

Similarly, for the staggered configurations it found that the temperature difference for the case I which equal to 40K is also better compared to the case II which is less than 20K. The same behavior for the cold fluid (water) can be concluded. In fact, this difference is 28 K for the case I, however it is drastically reduced to 7K for the case II (turbulent flow in staggered arrangement).

Furthermore, it is clear that the heat exchanger's design causes the cold fluid's temperature to fluctuate during the heat exchange with the tube containing the hot oil from the right side of the shell to the exit. As the cold fluid approaches and touches the tube, its temperature rises due to heat transfer through the tube wall. Simultaneously, the cold fluid then gradually cools within the bank tubes again as it moves away from the tube until it exits the shell. Simply, the hot liquid in the tube acts as the heat source for the cold fluid in the shell side of the heat exchanger, causing the cold fluid's temperature to increase and then decrease. This behavior is directly related to the nature of the boundary layer developing during the heat transfer between the two heat transfer fluids considered. A simple explanation is that when a fluid flows through a channel or on a surface, a thin layer is formed on the interface between the wall and the fluid. In this thin layer, fluid velocity changes from zero (static) at the wall surface to freestream velocity at a certain distance away from the wall surface. A thick boundary layer has a negative effect on heat exchanger performance as it impedes heat transfer. Think of it like a blanket, the thicker the blanket, the higher the insulation. This is not ideal for a heat exchanger device as the main objective is to conduct the maximum possible of heat between the two existing fluids via a tube surface and vice-versa. Turbulent flow is generally preferred in heat exchanger design. The swirling and diffusive characteristics of turbulent flow enhance heat transfer. Mixing induced by a turbulent flow can also disrupt the growth of the boundary layer on heat exchanger's inner surfaces. However, turbulent flow is often associated with higher pressure drop.

Based on these preliminary results, it seems that under these thermal and dynamic boundary conditions corresponding to the two chosen heat transfer fluids (water and oil), the laminar flow is more effective in transferring heat than the turbulent flow in both configurations. Moreover, in both cases the in-line arrangement clearly shows their efficiency in obtaining more heat transfer exchange compared to the staggered one. Furthermore, it is important to mention that despite the calculation was carried out in steady regime, these results can be attributed to the necessary time to ensure the desired thermal exchange which is not enough in the turbulent case, on one hand and the required size of the heat exchanger in terms of tubes length and number, on other hand.

III.2. Thermal balance

III.2.1. Heat transfer from a bank of tubes in cross flow heat exchanger

As well-known the dynamic configuration is a relevant factor in heat transfer to or from a bank (or bundle) of tubes in cross flow heat exchangers. The geometric arrangement chosen in our studied cases is shown schematically in Figure (III.4). As above mentioned, water

moves over the tubes, while oil at a different temperature passes through the tubes. In this section we are specifically interested in the effect of nature of low (laminar or turbulent) on the efficiency of heat gain in terms of the resulting convection heat transfer associated with cross flow over the tubes.

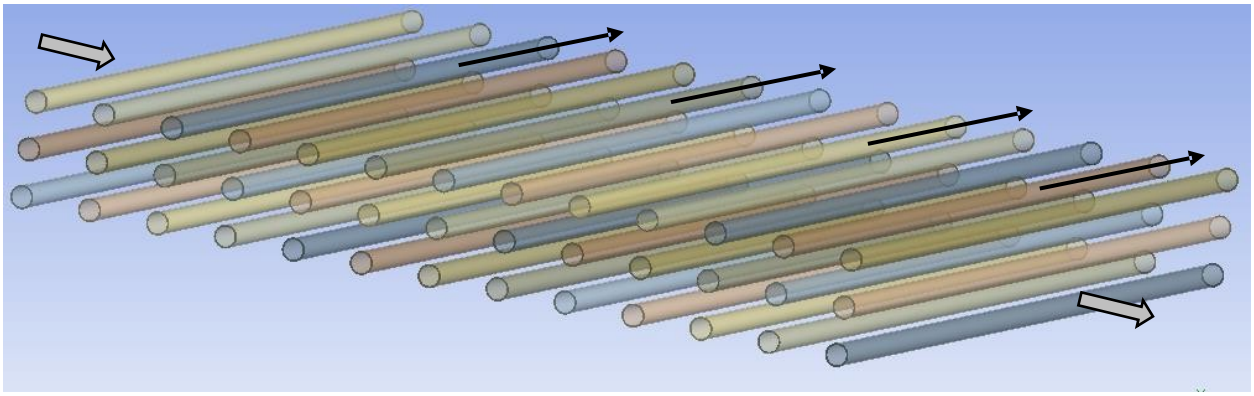

Figure III.4. *Schematic of a tube bank in cross flow Heat exchanger.*

In our study both aligned and staggered of tubes arrangement in the direction of the water flowing inside the shell with a typical velocity V, are considered (see Figure III.5). The configuration is characterized by the tube diameter D and by the transverse pitch S_T and longitudinal pitch S_L measured between tube centers.

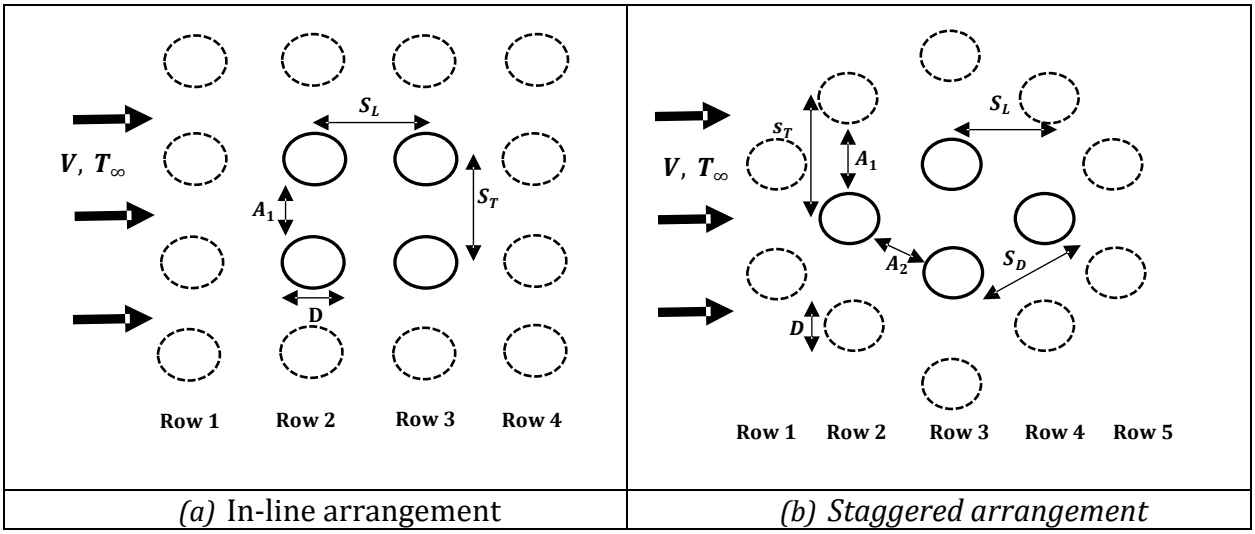

(a) In-line arrangement | *(b) Staggered arrangement*

Figure III.5. *Tube arrangements in a bank. (a) Aligned. (b) Staggered*

Flow conditions within the bank are dominated by boundary layer separation effects and by wake interactions, which in turn influence convection heat transfer. For downstream rows, flow conditions depend strongly on the tube bank arrangement (Figure III.6). Aligned tubes beyond the first row reside in the wakes of upstream tubes, and for moderate values of S_L convection coefficients associated with downstream rows are enhanced by mixing, or turbulation, of the flow. Typically, the convection coefficient of a row increases with

increasing row number until approximately the fifth row, after which there is little change in flow conditions and hence in the convection coefficient.

For our study (S_T = 50 mm and S_L = 75 mm ⇒ S_T/S_L = 0.67), thereby as widely reported in the heat transfer literature [1,2], this means that the influence of upstream rows decreases, and heat transfer in the downstream rows is not enhanced. For this reason, operation of aligned tube banks with S_T/S_L < 0.7, is undesirable.

Arrangement	Case I (laminar flow)	Case II (turbulent flow)
in-line	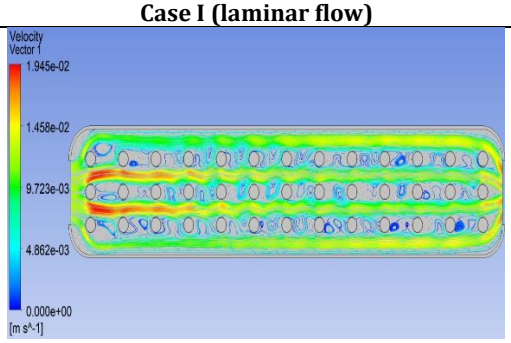 (a)	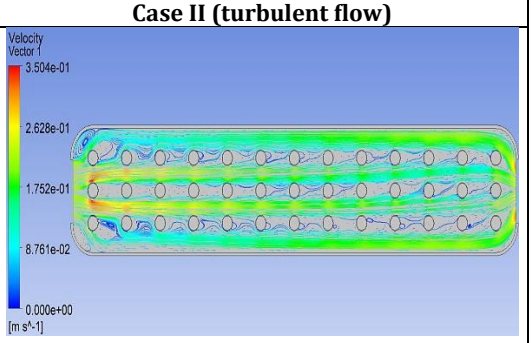 (b)
Staggered	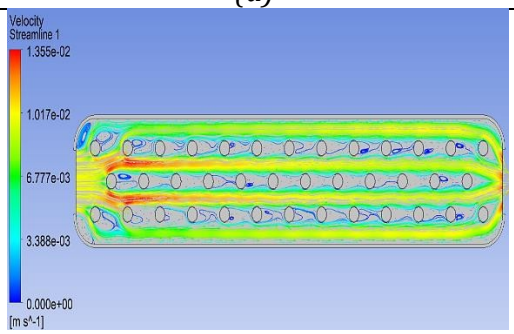 (c)	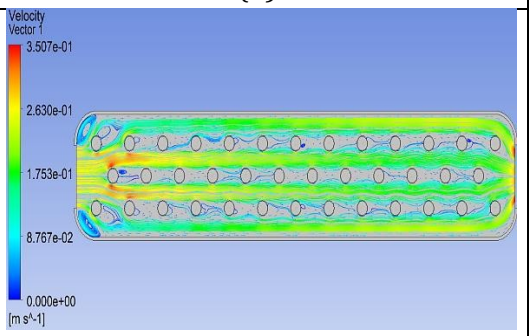 (d)

Figure III.6. *Cold fluid Streamlines of all cases.*

For the staggered tube array, the path of the main flow is more tortuous, and mixing of the cross-flowing fluid is increased relative to the aligned tube arrangement. In general, heat transfer enhancement is favored by the more tortuous flow of a staggered arrangement, particularly for small Reynolds numbers ($Re_D \leq 100$).

The Reynolds number $Re_{D,max}$ is based on the maximum fluid velocity occurring within the tube bank, $Re_{D,max} = \rho V_{max} D/\mu$. For the aligned arrangement, V_{max} occurs at the transverse plane A_1 of Figure (III.5-a), and from the mass conservation requirement for an incompressible fluid.

$$V_{max} = \frac{S_T}{S_T - D} V \qquad \textbf{(III.2)}$$

For the staggered configuration, the maximum velocity may occur at either the transverse plane A_1 or the diagonal plane A_2 of Figure (III.5-b). It will occur at A_2 if the rows are paced such that

$$2(S_D - D) < (S_T - D) \quad \textbf{(III.3)}$$

The factor of 2 results from the bifurcation experienced by the fluid moving from the A_1 to the A_2 planes. Hence V_{max} occurs at A_2 if [3]

$$S_D = [S_L^2 + (\frac{S_T}{2})^2] < \frac{S_T+D}{2} \quad \textbf{(III.4)}$$

in which case it is given by: [3]

$$V_{max} = \frac{S_T}{2(S_D-D)} V \quad \textbf{(III.5)}$$

If V_{max} occurs at A_1 for the staggered configuration, it may again be computed from the method given for aligned arrangement.

Since the fluid may experience a large change in temperature as it moves through the tube bank, the heat transfer rate could be significantly over predicted by using $\Delta T = (T_s - T_\infty)$ as the temperature difference in Newton's law of cooling. As the fluid moves through the bank, its temperature approaches T_s and $|\Delta T|$ decreases. The appropriate form of ΔT is shown to be a log-mean temperature difference, [3].

$$\Delta T_{lm} = \frac{(T_s-T_i)-(T_s-T_o)}{\ln(\frac{T_s-T_i}{T_s-T_o})} \quad \textbf{(III.6)}$$

Typically, we wish to know the average heat transfer coefficient for the entire tube bank. Zukauskas [3], has proposed a correlation of the form

$$Nu_D = 1.13 C_1 Re_{D,max}^m (Pr)^{0.36} \quad \begin{matrix} N_L \geq 20 \\ [\ 0.7 \leq Pr \leq 500\ ] \\ 10 \leq Re \leq 2 \times 10^6 \end{matrix} \quad \textbf{(III.7)}$$

where N_L is the number of tube rows, all properties are evaluated at the arithmetic mean of the fluid inlet ($T_i = T_\infty$) and outlet (T_o) temperatures, and the constants C_1 and m are listed in Table (III.2). The need to evaluate fluid properties at the arithmetic mean of the inlet and outlet temperatures is dictated by the fact that the fluid temperature will decrease or increase, respectively, due to heat transfer to or from the tubes.

Table III.2. *Constants of Equation (III.7) for the tube bank in cross flow, [03]*

Configuration	$Re_{D,max}^{mi}$	C_1	m
In-line	$10\text{-}10^2$	0.80	0.40
Staggered	$10\text{-}10^2$	0.90	0.40
In-line	$10^2\text{-}10^3$	Approximate as a single (isolated) cylinder	
Staggered	$10^2\text{-}10^3$		
In-line $(S_T/S_L)^a < 0.7$	$10^3 - 2\times10^5$	0.27	0.63
Staggered $(S_T/S_L) < 2$	$10^3 - 2\times10^5$	$0.35(S_T/S_L)^{1/5}$	0.60
Staggered $(S_T/S_L) > 2$	$2\times10^5 - 2\times10^6$	0.40	0.60
In-line	$2\times10^5 - 2\times10^6$	0.021	0.84
Staggered	$2\times10^5 - 2\times10^6$	0.021	0.84

If there are 20 or fewer rows of tubes, $N \leq 20$, the average heat transfer coefficient is typically reduced, and a correction factor may be applied such that

Table III.3. *Correction factor* C_2 *for* $N_L \leq 20, Re_{D,max} \geq 10^3$

N_L	1	2	3	4	5	7	10	13	16
In-Line	0.70	0.80	0.86	0.90	0.92	0.95	0.97	0.98	0.99
staggered	0.64	0.76	0.84	0.89	0.92	0.95	0.97	0.98	0.99

III.2.2. Heat transfer in the bundle of tubes of cross flow heat exchanger

When dealing with internal flows in bundle of tubes, it is important to be aware of the extent of the entry region, which depends on the flow regime, i.e. laminar or turbulent. The Reynolds number for flow in a circular tube is defined as: Kays et *al.* [4]

$$\boldsymbol{Re = \frac{DV\rho}{\mu} = \frac{DV}{\nu}} \qquad \textbf{(III.8)}$$

D is the inside diameter of the tube (or pipe), V is the average velocity of the fluid, ρ is the density of the fluid and μ is its dynamic viscosity. It is common to use the kinematic viscosity $\nu = \mu/\rho$ in defining the Reynolds number. Another common form involves using the mass flow rate $\dot{m}$ instead of the average velocity. the mass flow rate is related to the volumetric flow rate Q via $\dot{m} = \rho Q$ and we can write.

$$\boldsymbol{Q = \frac{\pi}{4} D^2 V} \qquad \textbf{(III.9)}$$

When the Reynolds number is ranging between $2300 < Re < 4000$. A correlation for the Nusselt number for laminar flow heat transfer was provided by Sieder-Tate equation:

$$\boldsymbol{Nu = 1.86 Re^{\frac{1}{3}} pr^{\frac{1}{3}} \left(\frac{D}{L}\right)^{\frac{1}{3}} \left(\frac{\mu_b}{\mu_w}\right)^{\left(\frac{1}{3}\right)}} \qquad \textbf{(III.10)}$$

III.2.2.1. The mean velocity

The velocity varies over the cross section and there is no well-defined free stream, it is necessary to work with a mean velocity um when dealing with internal flows. This velocity is defined such that, when multiplied by the fluid density and the cross-sectional area of the tube *Ac*, it provides the rate of mass flow through the tube. Hence,

$$\boldsymbol{\dot{m} = \rho u_m A_c} \qquad \textbf{(III.11)}$$

For steady, incompressible flow in a tube of uniform cross-sectional area, and u_m are constants independent of *x*. For flow in a circular tube in $A_c = \pi D^2/4$, the Reynolds number reduces to, [4].

$$\boldsymbol{Re_D = \frac{4Q}{\pi D v} = \frac{4\dot{m}}{\pi D \mu}} \qquad \textbf{(III.12)}$$

III.2.2.2. Friction factor

The engineer is frequently interested in the pressure drop needed to sustain an internal flow because this parameter determines pump or fan power requirements. for fully developed laminar flow:

$$\boldsymbol{f = \frac{64}{Re_D}} \qquad \textbf{(III.13)}$$

For fully developed turbulent flow, the analysis is much more complicated, and we must ultimately rely on experimental results. in addition to depending on the Reynolds number, the friction factor is a function of the tube surface condition and increases with surface roughness i.e, Measured friction factors covering a wide range of conditions have been correlated by Colebrook and are described by the transcendental expression:

$$\boldsymbol{\frac{1}{\sqrt{f}} = -2.0 \log\left[\frac{\frac{e}{D}}{3.7} + \frac{2.51}{Re_D\sqrt{f}}\right]} \qquad \textbf{(III.14)}$$

The pipe's relative roughness (e/D), where e is the pipe's effective roughness height and D the pipe (inside) diameter.

A correlation for the smooth surface condition that encompasses a large Reynolds number range has been developed by Petukhov and is of the form:

$$\boldsymbol{f = (0.790 ln Re_D - 1.64)^{-2}} \qquad \boldsymbol{3000 \leq Re_D \leq 5 \times 10^6} \qquad \textbf{(III.15)}$$

Another correlation giving excellent results on smooth surfaces is provided as below:

$$\begin{cases} f = 0.316 Re_D^{-\frac{1}{4}} & Re_D \leq 2.10^4 \\ f = 0.184 Re_D^{-\frac{1}{5}} & Re_D \geq 2.10^4 \end{cases} \quad \textbf{(III.16)}$$

One correlation for Nusselt number under turbulent flow in circular tubes, valid for smooth tubes over a large Reynolds number range including the transition region, is provided by Genilinski:

$$Nu = \frac{(\frac{f_c}{8})(Re-1000)pr}{1+12.7(\frac{f_c}{8})^{\frac{1}{2}}(pr^{\frac{2}{3}}-1)} \quad \textbf{(III.18)}$$

The correlation is valid for $0.5 \leq Pr \leq 2000$ and $3000 \leq Re_D \leq 5 \times 10^6$. in using this equation, which applies for both uniform surface heat flux and temperature, properties should be evaluated at mean temperature T_m.

III.2.3. Estimation of correction factor of cross flow heat exchanger

The correction factor (F) is used to adjust the idealized effectiveness to account for non-ideal conditions, which is influenced by the heat exchanger's shape as well as the temperatures of the hot and cold fluid streams at the intake and outflow. As shown in the figure below, the two temperature ratios P and R define the correction factor for our cross-flow heat exchanger configurations:

$$\begin{cases} P = \frac{t_2-t_1}{T_1-t_1} \\ R = \frac{T_2-T_1}{t_2-t_1} \end{cases} \quad \textbf{(III.19)}$$

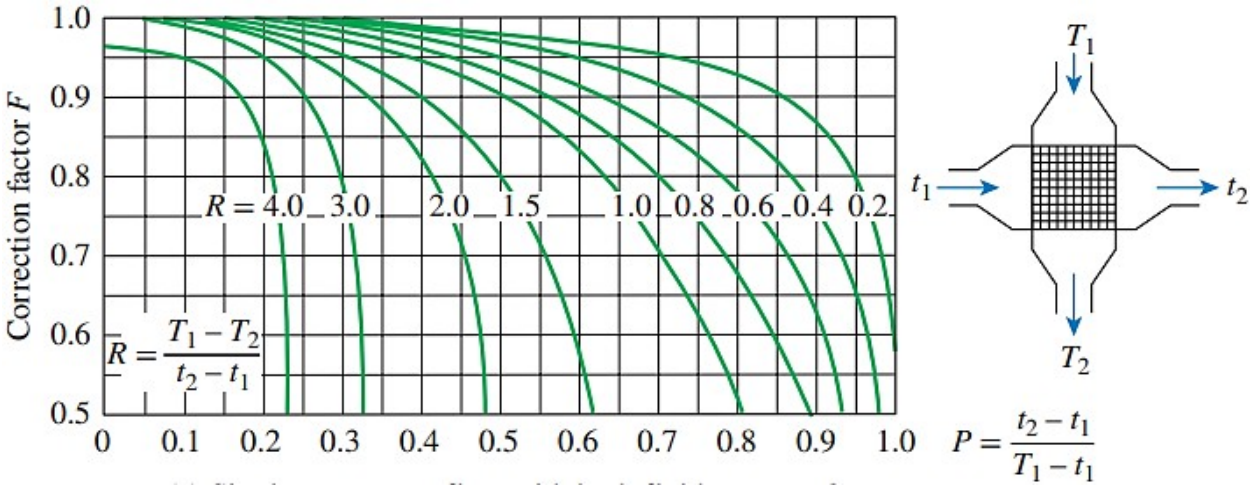

(a) Cross-flow with both fluids unmixed

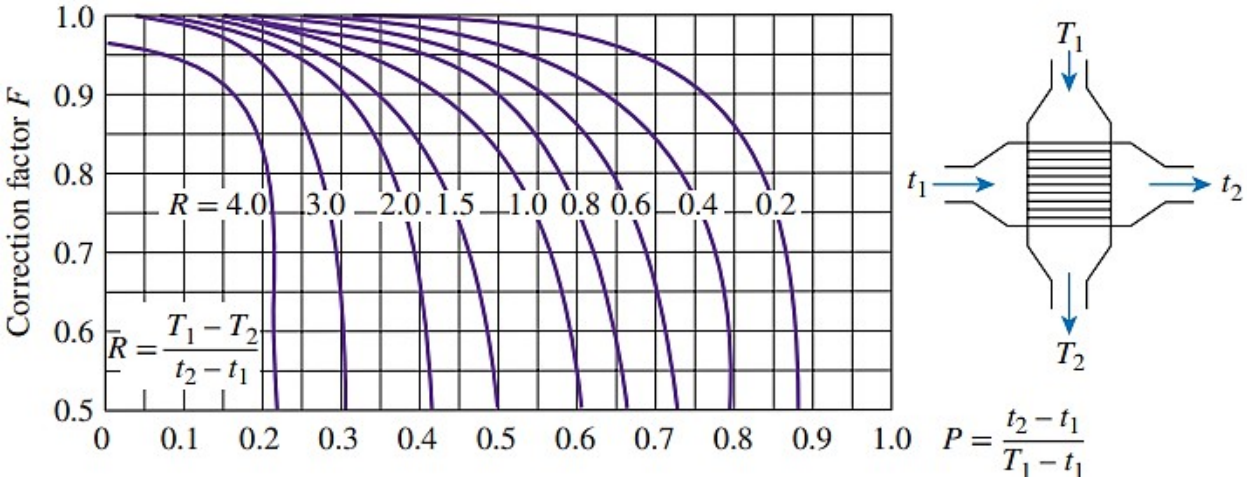

(b) Cross-flow with one fluid mixed and the other unmixed

Figure III.7. *Correction factor F charts for cross-flow heat exchangers.*

where the input and output are marked by "1" and "2", respectively. Notice that, according to the correction factor charts, "*T*" and "*t*", respectively, indicate the shell- and tube-side temperatures of a cross-flow heat exchanger.

The correction factor "*F*" for the most common shell and tube heat exchanger configurations is given in equation (III.20) in relation to two temperature ratios "*P*" and "*R*" defined as:

$$F = \frac{\frac{\sqrt{R^2+1}}{R-1} Ln\left(\frac{1-P}{1-P.R}\right)}{Ln\left(\frac{(2/P)-1-R+\sqrt{R^2+1}}{(2/P)-1-R-\sqrt{R^2+1}}\right)} \qquad \textbf{(III.20)}$$

III.2.4. The overall heat transfer coefficient:

A heat exchanger typically involves two flowing fluids separated by a solid wall. Heat is first transferred from the hot fluid to the wall by convection, through the wall by conduction, and from the wall to the cold fluid again by convection. Any radiation effects are usually included in the convection heat transfer coefficients. The thermal resistance network associated with this heat transfer process involves two convection and one conduction resistances, as shown in Figure (III.8). Here the subscripts "*i*" and "*o*" represent the inner and outer surfaces of the inner tube. For each pipe constituting the bundle of cross flow heat exchanger, we have $A_i = \pi D_i L$ and $A_o = \pi D_o L$, and the thermal resistance of the tube wall in this case is:

$$R_{wall} = \frac{Ln(D_o / D_i)}{2\pi\lambda L} \qquad \textbf{(III.21)}$$

where λ is the thermal conductivity of the wall material and L is the length of the tube. Then the total thermal resistance becomes:

$$R = R_{total} = R_{wall} = R_i + R_{wall} + R_o = \frac{1}{h_i A_i} + \frac{\ln(D_o / D_i)}{2\pi\lambda L} + \frac{1}{h_o A_o} \qquad \textbf{(III.22)}$$

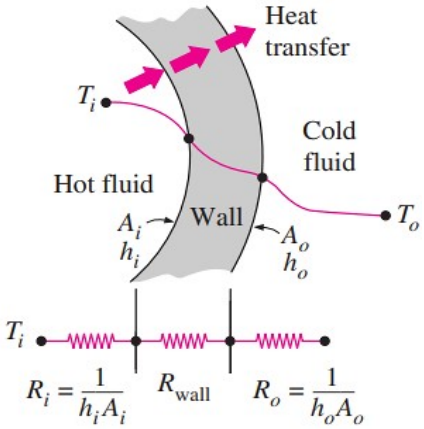

Figure III.8. *Thermal resistance network associated with heat transfer in each tube constituting the whole bundle of cross flow heat exchanger.*

The A_i is the area of the inner surface of the wall that separates the two fluids, and A_o is the area of the outer surface of the wall. In other words, A_i and A_o are surface areas of the separating wall wetted by the inner and the outer fluids, respectively.

In the analysis of heat exchangers, it is convenient to combine all the thermal resistances in the path of heat flow from the hot fluid to the cold one into a single resistance R, and to express the rate of heat transfer between the two fluids as:

$$Q = \frac{\Delta T}{R} = UA\,\Delta T = U_i A_i \Delta T = U_o A_o \Delta T \qquad \textbf{(III.23)}$$

where U is the overall heat transfer coefficient, which is identical to the unit of the ordinary convection coefficient h. Canceling ΔT, Eq. (III.23) reduces to:

$$\frac{1}{UA_s} = \frac{1}{U_i A_i} = \frac{1}{U_o A_o} = R = \frac{1}{h_i A_i} + R_{wall} + \frac{1}{h_o A_o} \qquad \textbf{(III.24)}$$

As the case of our geometry chosen (Di = 22mm and D_o = 24mm, i.e. δ = 1 mm), when the wall thickness of the bundle tubes is relatively small and the thermal conductivity of the tube material is high, as is the case of copper, the thermal resistance of the tube is negligible ($R_{wall} \simeq 0$) and the inner and outer surfaces of the tube are almost identical ($A_i = A_o = A_s$). Then equation (III.24) for the overall heat transfer coefficient simplifies to:

$$U \approx \frac{1}{\frac{1}{h_i} + \frac{1}{h_o}} \qquad \textbf{(III.25)}$$

where $U \simeq U_i \simeq U_o$. The individual convection heat transfer coefficients inside and outside the tube, h_i and h_o, are determined using the convection relations discussed in previous sections.

III.3. Estimation of the effectiveness of cross tube heat exchanger

The effectiveness of the heat exchanger represents the ratio of actual heat transfer to the maximum possible heat transfer. It can be calculated using:

$$\varepsilon = \frac{Q}{Q_{max}} = \frac{\textit{Actual heat transfer rate}}{\textit{Maximum possible heat transfer rate}} \qquad \textbf{(III.26)}$$

The actual heat transfer rate in a heat exchanger can be determined from an energy balance on the hot or cold fluids and can be expressed as:

$$Q = C_c(T_{c,out} - T_{c,in}) = C_h(T_{h,in} - T_{h,out}) \qquad \textbf{(III.27)}$$

Where $C_c = m_c \times Cp_c$ and $C_h = m_h \times Cp_h$ are the heat capacity rates of the cold and the hot fluids, respectively. To determine the maximum possible heat transfer rate in a heat exchanger, we first recognize that the maximum temperature difference in a heat exchanger is the difference between the inlet temperatures of the hot and cold fluids. That is,

$$\Delta T_{max} = T_{h,in} - T_{c,in} \qquad \textbf{(III.27)}$$

In fact, the heat transfer in a heat exchanger will reach its maximum value when (1) the cold fluid is heated to the inlet temperature of the hot fluid or (2) the hot fluid is cooled to the inlet temperature of the cold fluid. These two limiting conditions will not be reached simultaneously unless the heat capacity rates of the hot and cold fluids are identical (i.e., $C_c \neq C_h$). Therefore, the maximum possible heat transfer rate in a heat exchanger is:

$$Q_{max} = C_{min}\,\Delta T_{max} = C_{min}(T_{h,in} - T_{c,in}) \qquad \textbf{(III.28)}$$

Effectiveness relations of the heat exchangers typically involve the dimensionless group UA_s/C_{min}. This quantity is called the number of transfer units NTU and is expressed as:

$$\textbf{NTU} = UA_s/C_{min} \qquad \textbf{(III.29)}$$

In heat exchanger analysis, it is also convenient to define another dimensionless quantity called the capacity ratio c a:

$$c = \frac{C_{min}}{C_{max}} \qquad \textbf{(III.30)}$$

It can be shown that the effectiveness of a heat exchanger is a function of the number of transfer units NTU and the capacity ratio c. That is,

$\varepsilon = function\ (UA_s/C_{min},\ C_{min}/C_{max}) = function\ (NTU,\ c)$

Effectiveness relations have been developed for the case of crossflow heat exchangers, and the results are given in Table (III.4).

Table III.4. *Effectiveness relations for heat exchangers: NTU = UA_s/C_{min} and c = C_{min}/C_{max} = $(m.cp)_{min}/(m.cp)_{max}$, [5].*

Crossflow single-pass heat exchanger	
Both fluids unmixed	$\varepsilon = 1 - exp\ \{NTU^{0.22}\ .\ c.\ [exp(-c.\ NTU^{0.78}) - 1]\ \}$
C_{max} mixed, C_{min} unmixed	$\varepsilon\ =\ \frac{1}{c}\ (1 - exp\{-c[1 - exp(-NTU)]\})$
C_{min} mixed, C_{max} unmixed	$\varepsilon\ =\ 1 - exp\{-\frac{1}{c}[\ 1 - exp(-c.\ NTU)]\}$
Phase change (c=0)	$\varepsilon\ =\ 1 -\ exp(-NTU)$

The effectiveness's of this type of heat exchangers are also plotted in Fig. (III.9).

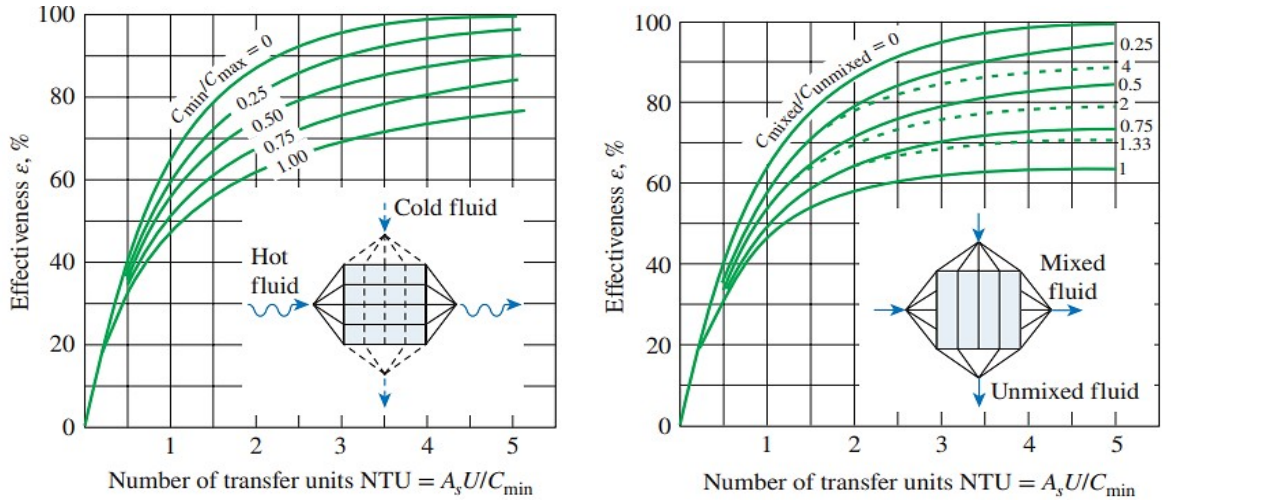

(a) Cross-flow with both fluids unmixed *(b) Cross-flow with one fluid mixed and the other unmixed*

FIGURE III.9. *Effectiveness for crossflow heat exchangers, [5].*

In the end, after we applied all the previous correlations and relationships to the four cases that we studied, the obtained results are reported in the Table (III.5).

	Case I				**Case II**			
	In-Line		Staggered		In-Line		Staggered	
	Pipe	Shell	Pipe	Shell	Pipe	Shell	Pipe	Shell
Re	15.62	229.23	15.62	114.6	312.4	4598.7	312.4	2299.4
Nu	24.7	15.89	24.7	13.98	67	110.5	67	68.5
h [W/m².°C]	247	397	247	343.66	670.57	2762	670.57	1713
F	0.945		0.951		0.9983		0.9981	
V_{max} [m/s]	0.01	0.0096	0.01	0.0048	0.2	0.192	0.2	0.096
***Q* [kW]**	46.1		44.2		287.9		255.7	
U [W/m². °C]	152.26		143.59		539.5		482	

Table III.5. *The final results obtained from both the numerical simulation and the theoretical calculation.*

III.4. Partial conclusion

As a result of the findings, which shows that the overall heat transfer coefficient in the in-line set arrangement is higher in both cases than in the staggered set arrangement, we can conclude that this type of heat exchanger have a better heat transfer performance and efficiency when the in-line pipe set arrangement is used.

REFERENCES:

[1] Knudsen, J. D., and D. L. Katz, "Fluid Dynamics and Heat Transfer", McGraw-Hill, New York, 1958.

[2] Jakob, M., Heat Transfer, Vol. 1, Wiley, New York, 1949. 14. Sparrow, E. M., J. P. Abraham, and J. C. K. Tong, Int. J. Heat Mass Transfer, 47, 5285, 2004.

[3] Zukauskas, A., "Heat Transfer from Tubes in Cross Flow," in J. P. Hartnett and T. F. Irvine, Jr., Eds., Advances in Heat Transfer, Vol. 8, Academic Press, New York, 1972.

[4] Kays, W.M., and London, A. "Basic Heat Transfer and Flow Friction Design Data for Gas Flow Normal to Banks of Staggered Tubes: Use of a Transient Technique", Stanford University. Department of Mechanical Engineering, 1952.

[5] W. M. Kays and A. L. London. Compact Heat Exchangers, 3^{edition}. McGraw-Hill, 1984.

General conclusion

A full 3D numerical was developed in order to investigate the main factors that have a direct impact in the thermal performances of a crossflow heat exchanger. The focus was to affect the of the type of arrangement, i.e. aligned or staggered as well as the flow regime in the shell on the heat exchanger effectiveness. Two coolants were chosen oil as unmixed hot fluid flows through the bundle of pipes and water as mixed cold fluid in the shell. Additionally, the impact of increasing velocity on the resulting global coefficient of heat transfer, was also examined.

Considering the outcomes we have found that the In-line pipe set arrangement is more thermally efficient than the staggered pipe set arrangement, due to the cold fluid heated more and the pipe walls cooled better in that configuration. Moreover, it is found that in the case II corresponding to the turbulent flow in both arrangements (In-line and staggered), the nature of flow around a tube in the second and subsequent rows is very different due to the wakes formed and the turbulence caused by the tubes upstream. Although, as well known the level of turbulence, and thus the heat transfer coefficient, increases with row number because of the combined effects of upstream rows, there is no significant change in turbulence level after the first few rows, and thus the heat transfer coefficient remains constant.

It is important to note that this preliminary study is by no means completed, as heat exchangers have diverse applications with specific requirements. For example, our study only explored the effects of keeping the nature of the cold liquid which is water in each case. However, further investigations can be conducted by reversing the water with oil or another liquid or changing both fluids' properties to evaluate their impact on thermal and dynamic parameters. Additionally, there are various geometries and setups to try, and the possibilities for optimizing heat exchangers and searching for better operational conditions are endless.

In conclusion, we hope that our work has met your expectations and contributed, even in a small way, to initiations of scientific research. We also hope that this experience has opened our eyes to higher academic and professional opportunities and that it can serve as a helpful resource for other students conducting similar studies.